

**PRETREATMENT OF SIMULATED TANNERY WASTEWATERS BY
SONICATION WITH NANOSCALE IRON PARTICLES**

by

Betül Aydın

BS. in Env.E. Uludag University, 2004

**Submitted to the Institute of Environmental Sciences in partial fulfillment of
the requirements for the degree of
Master of Science
in
Environmental Sciences**

Boğaziçi University

2009

**PRETREATMENT OF SIMULATED TANNERY WASTEWATERS BY
SONICATION WITH NANOSCALE IRON PARTICLES**

APPROVED BY:

Prof. Dr. Nilsun H. İnce

(Thesis Supervisor)

Prof. Dr. Ayşen Erdinçler

Prof. Dr. E. Beyza Üstün

DATE OF APPROVAL 10.06.2009

ACKNOWLEDGEMENTS

I would like to express my sincere gratitude to my thesis supervisor Prof. Dr. Nilsun H. İnce for her support, valuable guidance and endless patience throughout this study.

I am also thankful to my jury members Prof. Dr. Ayşen Erdiñler and Prof. Dr. E. Beyza Üstün for their critical and supportive comments.

I would like to thank Gülhan Özkösemen and Mehmet Ali Küçüker for their help during my laboratory studies. I wish to express my thanks to Işıl Gültekin and Asu Ziyilan for their motivation and encouragement.

I want also to express my gratitude to my dear parents, Gülizar and Ömer Aydın, my brother Murat and my sisters Gülçin, Esra, Kübra and Zeynep for their love, encouragement and endless support throughout my life.

Lastly, I would like to express my gratitude and thanks to Taner Hoccođlu whose love and encouragement always make me feel in confidence.

ABSTRACT

Radiation processes (RP) have emerged as innovative ultimate treatment technologies for water and wastewater remediation. The advantage over conventional processes is due to their capacity to convert pollutants to simple elemental constituents without transferring them to another phase, as is the case in stripping, precipitation and carbon filtration. Recent research has shown that Nanoscale particles have been demonstrated to be very effective for the transformation and detoxification of a wide variety of common environmental contaminants.

The purpose of this research was to investigate treatability of chromium(III) by adsorption on nanoscale iron particles and the enhancement in the process by sonication of the solution. Selection of Cr(III) was based on the fact that it is the major pollutant in tannery wastewater and very toxic.

Experiments with nanoparticles to assess the adsorptive properties of the chromium followed by combined processes involving the particles and ultrasound. All those experiments were run to investigate the impacts of operational parameters such as adsorbent concentration, pH and contact time. It was found that the rate of destruction of the chromium by adsorption and ultrasound followed pseudo-first order kinetics. The results have shown that the use of ultrasound in presence of nanoparticles significantly enhanced the degradation duration.

Overall, this study has demonstrated that chromium in tannery wastewaters may be effectively destroyed by use of optimized hybrid processes involving ultrasound and nanoparticles.

ÖZET

Radyasyon süreçleri (RP) su ve atıksu arıtımında nihai arıtma teknolojileri olarak ortaya çıkmıştır. Geleneksel süreçler ile karşılaştırıldığında en önemli avantajı kirleticileri başka bir faza transfer etmeden basit elementel birleşenlere dönüştürmesidir. Son zamanlarda yapılan araştırmalar, nanopartiküllerin birçok çevre kirleticilerin transformasyonunda ve detoksifikasyonunda çok etkili olduğunu göstermektedir.

Bu araştırmanın amacı; kromun sesüstü dalgalar, nanopartiküller ve hybrid sistemler ile parçalanmasının araştırılmasıdır. Deri endüstrisi atıksularında ana kirletici olması ve toksik özelliği nedeni ile yapılan deneylerde kromun arıtılması üzerinde durulmuştur.

Nanopartiküller ile yapılan deneyler, hedef kirletici olan kromun adsorpsiyon kapasitesinin değerlendirilmesi ve bu partiküllerin sesüstü dalgalar ile birlikte kullanılmasından oluşmaktadır. Yapılan tüm deneylerde adsorban konsantrasyonu, pH ve temas süresi gibi operasyonel parametrelerin kromun arıtılması üzerindeki etkileri araştırılmıştır. Yapılan deneylerde kromun 1.derece reaksiyon kinetiğini takip ettiği tespit edilmiştir. Ses üstü dalgaların kullanılmasının en önemli etkisi kromun arıtılması için gerekli olan optimum temas süresini azaltmış olmasıdır.

Sonuç olarak, bu çalışma operasyonel parametrelerin optimizasyonu ile özellikle hibrid sistemler kullanıldığında deri endüstrisi atıksularında bulunan kromun etkin arıtımının sağlandığını ortaya koymaktadır.

TABLE OF CONTENTS

ACKNOWLEDGEMENT	iii
ABSTRACT	iv
ÖZET	v
TABLE OF CONTENTS	vi
LIST OF FIGURES	ix
LIST OF TABLES	xii
LIST OF SYMBOLS/ABBREVIATIONS	xiv
1. INTRODUCTION	1
2. THEORETICAL BACKGROUND	3
2.1. Overview of Leather Industry	3
2.1.1. Raw Hide Storage and Beam House Operations	5
2.1.1.1. Raw Hide Storage	5
2.1.1.2. The Beam House Operations	6
2.1.2. Tanyard Operations	7
2.1.3. Post-Tanning Operations	8
2.1.4. Finishing Operations	11
2.2. Environmental Relevance of Leather Tanning Industry	12
2.3. Adsorption	15
2.3.1. Types of Adsorption	15
2.3.2. Adsorption Isotherms	17
2.3.2.1. Freundlich Isotherm	17
2.3.2.2. Langmuir Isotherm	18
2.3.2.3. B.E.T. Equation	19
2.3.3. Factors Influencing Adsorption	19
2.3.3.1. Surface Area	19
2.3.3.2. Nature of the Adsorbate	20
2.3.3.3. pH	21
2.3.3.4. Temperature	21
2.4. Nanoscale Particles and Nanotechnology	22
2.4.1. The Fate of Nanoparticles in Water	24
2.4.2. Nanoscale Particals' Use in Wet Remediation	25

2.5.	Ultrasound	27
2.5.1.	Ultrasonically-Induced Cavitation	27
2.5.2.	Possible Reaction Sites in the Cavitation Process	29
2.5.3.	Parameters Affecting Sonochemical Reaction Systems	30
2.5.3.1.	Frequency	31
2.5.3.2.	Properties of the Solute	31
2.5.3.3.	Applied Pressure	31
2.5.3.4.	Properties of the Solvent	32
2.5.3.5.	Solids as Catalysts	32
2.5.3.6.	Properties of Saturating Gas	32
2.5.3.7.	Power Intensity	33
2.5.3.8.	Temperature	33
2.5.4.	Application of Ultrasound in Decontaminating Tannery Wastewater	34
3.	MATERIALS AND METHODS	35
3.1.	Materials	35
3.1.1.	Chemicals Used in Experiments	35
3.1.2.	Experimental Setup	36
3.1.2.1.	Horizontal Shaker	36
3.1.2.2.	Sonication experiments	37
3.2.	Methods	38
3.2.1.	Preparation of the Test Solutions.	38
3.2.2.	Adsorption Experiments	38
3.2.3.	Sonication Experiments	39
3.3.	Analytical Methods	39
4.	RESULTS AND DISCUSSION	41
4.1.	Adsorption of Chromium on Reactive Nanoscale Iron Particles	41
4.1.1.	Effect of Adsorbent Concentration	41
4.1.2.	Selection of the Isotherms	43
4.1.3.	Effect of Contact Time	46
4.1.4.	Effect of pH	47
4.1.5.	The Rate of Chromium Removal	48
4.2.	Adsorption of Chromium on H-200 Zero Valent Iron Suspension	50
4.1.1.	Effect of Adsorbent Concentration	50

4.1.2. Selection of the Isotherms	51
4.1.3. Effect of Contact Time	54
4.1.4. Effect of pH	54
4.1.5. The Rate of Chromium Removal	55
4.1.6. Effect of Solution Matrix 1	57
4.3. Ultrasound and Nanoparticles	58
4.3.1. Determination of Operational Parameters for RNIP	59
4.3.1.1. pH	59
4.3.1.2. Contact Time	60
4.3.2. Determination of Operational Parameters for H-200 Zero-Valent Iron	61
4.3.2.1. pH	62
4.3.2.2. Contact Time	63
4.3.2.3. Effect of Solution Matrix 1	64
4.4. Comparison of Silent and Sonicated Adsorption Systems	65
4.5. Comparison of Silent and Sonicated System (Solution Matrix 1)	67
4.6. Comparison of Silent and Sonicated System (Solution Matrix 2)	68
5. CONCLUSIONS	70
REFERENCES	72
APPENDIX A (Calibration Curve of Chromium for AAS Analysis)	78
APPENDIX B (Calibration Curve of COD for Spectrophotometer Analysis)	79

LIST OF FIGURES

Figure 2.1.	The scale of objects in the nanometer range	22
Figure 2.2.	Formation, growth and implosion of a cavitation bubble	27
Figure 2.3.	Possible sites of chemical reactions in homogeneous reaction media	29
Figure 3.1.	Photograph of horizontal shaker	30
Figure 3.2.	Photograph of 20 kHz probe inserted reactor	37
Figure 3.3.	Photograph of atomic absorption spectrometry	39
Figure 3.4.	Photograph of spectrophotometer	40
Figure 4.1.	Determination of optimum RNIP concentration	42
Figure 4.2.	Effect of RNIP concentration on the fraction of Cr(III) Removal	42
Figure 4.3.a.	Adsorption of Cr(III) on RNIP and the linearized best fit Freundlich Isotherm	44
Figure 4.3.b.	Adsorption of Cr(III) on RNIP and the linearized best fit Langmuir Isotherm	45
Figure 4.4.	Optimization of contact time for Cr(III) adsorption on RNIP	46
Figure 4.5.	Effect of pH on the adsorption of chromium on RNIP	47

Figure 4.6.	Speciation diagram for Cr(III) complexes present in aqueous Solution	48
Figure 4.7.	Estimation of the decay rate coefficients for chromium (pH: 5 RNIP: 20 mg L ⁻¹)	49
Figure 4.8.	Determination of optimum ZVI concentration	50
Figure 4.9.	Effect of ZVI concentration on the fraction of chromium removal	51
Figure 4.10.a.	Adsorption of chromium on ZVI and the linearized best fit Freundlich Isotherm.	52
Figure 4.10.b.	Adsorption of chromium on ZVI and the linearized best fit Langmuir Isotherm.	52
Figure 4.11.	Optimization of contact time for Cr(III) adsorption on ZVI	54
Figure 4.12.	Effect of pH on adsorption of chromium on ZVI	55
Figure 4.13.	Estimation of the decay rate coefficients for chromium (pH: 4 ZVI: 0.6 mg L ⁻¹)	56
Figure 4.14.	Fractions of chromium and BOD ₅ removal by adsorption in the presence of ZVI (pH:4, time: 2 hour)	57
Figure 4.15.	Effect of pH on chromium removal by ultrasound in the presence of RNIP	59
Figure 4.16.	Optimization of contact time for Cr(III) removal by ultrasound in the presence of RNIP (20 g L ⁻¹)	60

Figure 4.17. Effect of pH on the fraction of chromium removal by ultrasound in the presence of ZVI	62
Figure 4.18. Optimization of contact time for Cr(III) removal by ultrasound in the presence of ZVI	63
Figure 4.19. The fraction of chromium and BOD ₅ removal by ultrasound in the presence of ZVI	64
Figure A. Calibration curve of chromium for AAS analysis.	78
Figure B. Calibration curve of KHP solution for COD analysis.	79

LIST OF TABLES

Table 2.1.	Leather manufacturing processes and generated wastes	4
Table 2.2.	General characteristics of tannery wastewater	13
Table 2.3.	Discharge limits for leather processing industry effluents	14
Table 4.1.	Freundlich and Langmuir constants for chromium in the presence of RNIP	45
Table 4.2.	Chromium removal rate constant and the related statistical parameters (in the presence of RNIP)	49
Table 4.3.	Freundlich and Langmuir constants for chromium in the presence of ZVI.	53
Table 4.4.	Chromium removal rate constant and the related statistical parameters (in the presence of ZVI)	56
Table 4.5.	Operating parameters considered in the application of sonication to chromium	58
Table 4.6.	Operational Parameters for chromium (III) removal by adsorption of single solution in the presence of RNIP and ZVI	65
Table 4.7.	Operational Parameters for chromium (III) removal by sonication of single solution in the presence of RNIP and ZVI	66
Table 4.8.	The fraction of chromium and BOD ₅ removal by adsorption of solution matrix 1 (pH:4, ZVI: 0.6 g/L, t: 2 hour)	67

Table 4.9.	The fraction of chromium and BOD ₅ removal by sonication of solution matrix 1 (pH:4, ZVI: 0.6 g/L, t: 20 m)	67
Table 4.10.	The percentage of chromium, COD and BOD ₅ removal by adsorption of solution matrix 2 (pH:4, ZVI: 0.6 g L ⁻¹)	68
Table 4.11.	The percentage of chromium, COD and BOD ₅ removal by sonication of solution matrix 2 (pH: 4, ZVI: 0.6 g L ⁻¹)	69
Table A	Detected peak areas for the injected chromium solutions during calibration of AAS.	78
Table B	Detected peak areas for the injected KHP solutions during calibration of spectrophotometer.	79

LIST OF SYMBOLS/ABBREVIATIONS

Symbol	Explanation	Units used
k	Decay rate constant	s^{-1}
RNIP	Reactive Nanoscale Iron Particle	-
ZVI	Zero-Valent Iron	-
COD	Chemical Oxygen Demand	$(mg L^{-1})$
BOD ₅	5-day Biochemical Oxygen Demand	$(mg L^{-1})$

1. INTRODUCTION

Radiation processes (RP) have emerged as innovative ultimate treatment technologies for water and wastewater remediation. The advantage over conventional processes is due to their capacity to convert pollutants to simple elemental constituents without transferring them to another phase, as is the case in stripping, precipitation and carbon filtration. RPs use either free radicals such as OH to oxidize organic matter and other species, and/or the solvated electron (e_{aq}^-) or hydrogen atom to reduce oxidized species. An excellent source of e_{aq}^- and hydrogen atom is ionizing radiation, while a cost-effective method of generating OH and H radicals is ultrasound, which not only promotes aqueous phase oxidation, but also offers an excellent medium for thermal decomposition of contaminants in the gas phase (Ince et al., 2001).

The leather processing industry produces one of the most complex industrial wastewaters as a consequence of the miscellaneous structure and high concentration of the pollutants generated. The leather industry produces effluents containing more than one hundred different organic and inorganic chemicals, heavy metal salts, soaps, oils, waxes, solvents, dyes, etc. Chromium salts, chlorides (NaCl and NH_4Cl) and sulfur compounds (sulfides and sulfates) are the main pollutants released with process effluents.

Conventional methods of treatment for leather processing industry wastewaters are usually applied to the mixture of effluents from all process operations. The methods are based on physicochemical treatment followed by biological and advanced tertiary treatment. Therefore, commercial treatment plants are robust, require considerable consumption of chemical reagents, which not only result in an additional pollution source, but also make the system cost-ineffective.

Alternative methods of treating wastewaters of this type are still in the phase of investigation, with number of problems to be solved. In studies reported in the literature on such alternate solutions, it is found that in general only one pollution component (mainly chromium) is considered, so that much research is required for practicality of these solutions.

The purpose of this research was to investigate treatability of chromium(III) by adsorption on nanoscale iron particles and the enhancement in the process by sonication of the solution. Selection of Cr(III) was based on the fact that it is the major pollutant in tannery wastewater and very toxic.

Tanning wastewater was simulated by the addition of Cr^{3+} (40 mg L^{-1}), BOD_5 (400 mg L^{-1}) and COD (1000 mg L^{-1}). Two types of BOD_5 and COD were added, as glucose and pluck.

2. THEORETICAL BACKGROUND

2.1. Overview of Leather Industry

The leather processing industry produces one of the most complex industrial wastewaters as a consequence of the miscellaneous structure and high concentration of the pollutants generated. The leather industry produces effluents containing more than one hundred different organic and inorganic chemicals, heavy metal salts, soaps, oils, waxes, solvents, dyes, etc. Chromium salts, chlorides (NaCl and NH₄Cl) and sulphur compounds (sulphides and sulphates) are the main pollutants released with process effluents.

In the tanning process, animal hides and skins are treated to remove hair and non-structured proteins and fats, leaving an essentially pure collagen matrix. The hides than preserved by impregnation with tanning which give leather its stability and essential character. Leather manufacturing processes and generated wastes are summarized in Table 2.1, respectively.

Leather production usually involves four distinct phases (World Bank Group, 2000).

- Raw hidden storage and beam house operations
- Tanyard operations
- Post-tanning operations
- Finishing operations

Table 2.1 Leather manufacturing processes and generated wastes

Section	Operation	Source of Waste Generation	Nature of Waste
Beamhouse	Soaking	Soaking	Wastewater
	Pasting	Spills	Wastewater
	Liming	Spent lime liquor, lime mud	Wastewater, solid
	Fleshing	Cooling water, fleshing	Wastewater, solid
	De-liming, bating and degreasing	Spent liquor, wash streams, chemical spills	Wastewater, ammonia emissions
Tanning/Post Tanning	Pickling	Spent pickling bath	Wastewater
	Chrome tanning	Spent pickling bath, wash streams	Wastewater
	Sammying	Squeezed liquor	Wastewater
	Splitting	Splitting	Solid
	Shaving	Shavings	Air particulate emissions, solid
	Wetting	Spent wetting liquor	Wastewater
	Re-tanning	Spent re-tanning stream, wash streams	Wastewater
	Neutralization dyeing and fat liquoring	Spent liquor, spent dye bath, wash streams	Wastewater
	Sammying	Squeeze water	Wastewater
Finishing	Drying	Fugitive	Water vapour
	Trimming	Trimmings	Solid
	Buffing	Buffing dust	Air particulates
	Colour/ lacquer	Fugitive	Air

2.1.1. Raw Hide Storage and Beam House Operations

2.1.1.1. Raw Hide Storage. When the raw hides arrive at the tannery they are in a salted, chilled or dried condition to avoid decomposition of the hides. If they are chilled they have to be stored in a cold room and they should be processed within a few weeks. Most hides, however, are received as salted hides with a salt content of approximately 20 per cent salt.

Salted hides can be stored for a long period without impairing the quality of the leather. Processing of dried hides is not common. If the hides are received as fresh, then the processing has to be started within two days.

Properly handled fresh or chilled hides give the best quality and have the lowest negative environmental impacts. Salted hides give a good quality, but have adverse environmental impacts if the wastewater is discharged to freshwater rivers and lakes (COWI, 2000).

Following the raw hide storage, the hides are subjected to beam house operations. In the beam house process, unwanted parts such as hair, skin, etc. are removed from raw hides. The raw hides are prepared for the subsequent tanning process.

The wastewater from this process is characterized by high alkalinity and contains high concentration of both suspended solids (skin, hair-mud) and oil/grease. In addition, chemicals used in this production step, such as lime, soap, ammonium salts, alkaline, sulphide and bactericide are discharged with the beam house wastewater (GTZ, 1997).

2.1.1.2. The Beam House Operations.

Soaking

The main purposes of soaking are to re-hydrate the hide; and to remove manure, dirt and blood from the surface of the hide. Soaking is carried out in paddles, drums or mixers. The hides are typically washed for about one hour to remove dirt and salt. Then, a six hours or longer washing follows where wetting agents are added (COWI, 2000).

Depending on the type of raw materials used, soaking additives can be used such as surfactants, enzyme preparations and bactericides (European Commission, 2003). Chemicals used in soaking are 0.2-2.0 grams per liter sodium hydroxide, up to 1 gram per liter sodium hypochlorite and/or 0.5-2.0 per cent wetting agents, emulsifiers, surfactants.

Liming and Unhairing

The main purpose of liming and unhairing is to eliminate keratinous material (hairs, hair roots and epidermis) from the hides. Chemicals generally used are 2-10 per cent calcium hydroxide (lime), 1-4 per cent sodium sulphide or sodium hydrogen sulphide. Some caustic soda may also be used (National Cleaner Production Centre). Chemicals soften and dissolve the hair, so it can easily be washed off the hides. The processing time depends on the concentration of the chemicals (COWI, 2000).

Fleshing

Fleshing is a mechanical scraping of the excessive organic material from the hide (connective tissue, fat, etc.). The hides are carried through rollers and across rotating spiral blades by the fleshing machine (European Commission, 2003).

2.1.2. Tanyard Operations

In the tanyard the “pelt” (the hide at this stage) substance (collagen) is treated with chemicals which crosslink the collagen molecule to form a stable material (leather).

Deliming

The purpose of deliming is partially to neutralise the pelts in order to remove surplus lime, suppress the alkaline swelling and adjust the pH to the optimum value for the bating process. Deliming is typically carried out using ammonium chloride or ammonium sulphate, along with 0.5-2.0 per cent acids (lactic, formic, boric and mixtures) and acidic salts.

Bating

Bating is an enzymatic process that loosens the pelt structure and removes unwanted proteins prior to tanning. Normally the bating is carried out in the delimiting liquor (consumed process water/wastewater). The traditional bating enzyme preparations consist of a small amount of enzyme diluted in ammonium sulphate (or chloride) and sawdust (COWI, 2000). In this process the rest of the unwanted hair roots can be removed (Sharphouse, 1971).

The chemical used is often a 0.5 per cent bating material, which consists of 50 per cent wood flour (or another carrier), 30 per cent de-limiting agent (ammonium chloride) and 1-5 per cent pancreatic enzyme (National Cleaner Production Centre).

Pickling

Pickling brings the pelt to the desired pH for tanning and prevents swelling of the pelt. Chemicals used are 0.2-2.02 per cent sulphuric or formic acid and 6-10 per cent salt. Pickling is carried out in the tanning drum.

Tanning

Tanning is the stabilization of the collagen structure of the pelt using natural or synthetic chemicals. The various agents can be categorised in three main groups which are mineral tannages, vegetable tannins and alternative tanning agents, like syntants, aldehydes and oil tannage (HMIP, 1995).

Chromium tanning is more popular, because it is faster and cheaper. In addition, the chromium-tanned leather is more resistant to heat and humidity (GTZ, 1997). The most commonly used tanning agent is a basic chromium sulphate (approximately 80 per cent of the leather production in the world is chromium tanned). In chromium tanning about 6-10 per cent (with respect to pelt weight) of chromium powder containing 26 per cent chromium oxide (Cr_2O_3) is added.

Depending on the thickness of the pelt, tanning takes 6-10 hours. When the endpoint for chromium cross-linking has been reached, basification is achieved by gradually adding sodium bicarbonate until a pH of 4-4.3 is reached. During basification the temperature is raised to 40-45 °C to improve the chromium exhaustion (COWI, 2000).

2.1.3. Post-Tanning Operations

The wet and dry post-tanning operations adjust the leather properties. Splitting can be carried out at this stage, but it will increase the amount of chromium containing waste and prolong the time required for tanning.

Sammying

In the sammying operation the tanned pelt is brought to a uniform semi-dewatered state. The machine squeezes out surplus water of the pelt.

Splitting

By mechanical splitting the thickness of pelts is regulated and they are split horizontally into 2 layers. After the pelt is split, the top part, called “grain”, is used for production of finished leather. The lower part is called “split” (GTZ, 1997). Splitting is carried out on splitting machines, fitted with a band knife (European Commission, 2003).

Splitting can be done after liming and un-hairing or after chromium tanning, in the wet blue condition. In recent years, however, there has been a tendency towards lime splitting because of environmental considerations and reduced consumption of tanning agents.

Shaving

The shaving process is a mechanical regulation that is carried out to achieve an even thickness throughout the pelt. Shaving is carried out where minor adjustments to the thickness are required (Heidemann, 1993).

The pelts at this stage are called “**wet-blue**” which means chromium-tanned grain that is ready for wet post-tanning. Wet-blues are also tradable products. The wet post-tanning consists of neutralisation, retanning, dyeing and fat liquoring.

Neutralization

The neutralization is done in order to de-acidify the wet blue. Neutralisation is the process by which the wet-blue are brought to a pH suitable for the process of re-tanning , dyeing and fat liquoring (Heidemann, 1993).

Retanning

Re-tanning is usually carried out for wet-blue to improve its quality according to the market requirements. In this step the chemical used may be chromium, tanning or syntan (a synthetic chemical). The re-tanning comprises a supplementary tannage and gives the wet-blue its final properties.

Dyeing

Dyeing may or may not be carried out depending on the market demand. The dyeing process itself depends on the type of dye used. Normally formic acid is used for pH adjustment before dyeing. Up-take of dyes on the wet-blue is facilitated at increased temperature. Steam is usually used to heat up the wet-blue and the dyeing liquor (process water) (GTZ, 1997).

Fat Liquoring

Fat liquoring is done to obtain soft leather (COWI, 2000). Wet-blues must be lubricated to achieve product-specific characteristics and re-establish the fat content lost in the previous procedures. The oils used may be of animal or vegetable origin, or might be synthetics based on mineral oils.

Drying

The objective of drying is to dry the wet-blue in order to optimise the quality and area yield of the leather. There is a wide range of drying techniques and some may be used in combination. Each technique has a specific influence on the characteristics of the leather. Drying techniques include sammying, setting, centrifuging, hang drying, vacuum drying, toggle drying and paste drying. After drying, the leather may be referred to as "crust". Crust is a tradable intermediate product (HMIP, 1995).

2.1.4. Finishing Operations

The finishing operation is used in order to give the leather surface properties suitable for its intended end use.

Buffing and Trimming

The crust is in some cases buffed to give a smooth surface. The crust is trimmed to remove cuts or thick parts at the edge.

Finishing

The finishing layer determines the aesthetic qualities of the leather and imparts to the leather the necessary resistance towards wear and other influences (COWI, 2000).

The following list of operations includes commonly used mechanical finishing operations:

- Conditioning (optimising the moisture content in crust for subsequent operations)
- Staking (softening and stretching of crust)
- Buffing/dedusting (abrading of the crust surface and removing the resulting dust)
- Dry milling (mechanical softening)
- Polishing
- Plating/embossing (flattening or printing a pattern into the crust).

2.2. Environmental Relevance of Leather Tanning Industry

Wastewaters from leather industry are known to be heavily contaminated with inorganic and organic pollutants. The major environmental issue for the tannery is the extensive use of chromium tanning salts and the workers' direct contact with these toxic materials (Zhao et al., 2004).

Of world tanneries, 80-95 per cent use chromium (III) salts in their tanning processes. Chromium will only exist in the environment in the trivalent stage. In soil, chromium (VI) is rapidly reduced to chromium (III) by its oxidative action upon organic material (Donmez, 1989, Pearson, et al., 1999). Despite the fact that chromium has been under pressure from some regulatory authorities, the extent of substitution of chromium tanning agents has been limited. The main reason for this is that chromium is the most efficient tanning agent available, and it is relatively cheap.

About 20-25 per cent of the raw (salted) bovine hide weight is transformed to leather in the tanning process. In a conventional process, the majority of the weight is discharged in various types of wastes. In general, one tonne of raw hides generates approximately 600 kg of solid waste and 15-50 m³ of effluent containing about 250 kg COD and 100 kg BOD. The quantities and qualities of emissions and waste produced by tanneries strongly depend on the type of leather processed, the source of hides and skins and the techniques applied (Higham, 1994).

When there is neither control nor awareness on the part of tanneries, the diverse environmental impacts of the tanneries will affect many parameters including the surface water, soil, ground water, air and waste management systems.

A further aspect to be aware of in tanneries is the potential hazard to human health and the environment from handling, storing, transporting and packaging of chemicals. Furthermore, contamination of soil and groundwater may be caused through accidental releases, spillages and leakages of certain agents as well as by the treatment of effluents and wastes.

The general characteristics of (untreated) tannery wastewater are represented in Table 2.2 (Raghava et al., 2003). It is evident that the wastewater from tannery is highly polluting in terms of total suspended solids and chromium. The discharge of untreated wastewater not only makes the soil non-productive but also pollutes surface and groundwater.

Table 2.2. General characteristics of tannery wastewater

COD (mg/L)	BOD (mg/L)	Total Suspended Solids (mg/L)	Total Chromium (mg/L)
2500-8000	1000-3000	15.000-25.000	100-250

The discharge standards are due to the “Water Pollution Control Regulations” of Turkey for leather industry are given in Table 2.3. (Official Gazette, 1999).

Table 2.3. Discharge limits for leather processing industry effluents (Water Pollution Control Regulations of Turkey, 1999)

Parameter	Concentration	
	Values for 2 hours	Values for 24 hours
pH	6-9	6-9
BOD (mg/L)	150	100
COD (mg/L)	300	200
Sulfur (mg/L)	2	1
Chromium(III) (mg/L)	-	-
Chromium(VI) (mg/L)	0,5	0,3
Total Chromium (mg/L)	3	2
Total Suspended Solids (mg/L)	125	-
Oil and Grease (mg/L)	30	20
Toxicity Factor	4	4

Pollution from tanneries has a negative long-term impact on the growth potential of a country, irrespective of the immediate economic benefits of production. Polluted water, air or soil affects people's health, and damages the ecological processes that sustain the production of food. As a result, environmental issues have come to be relatively more important (UNEP, 1991).

2.3. Adsorption

Adsorption is the accumulation of a substance at or near an interface relative to its concentration in the bulk solution. The molecule that accumulates or adsorbs, at the interface is called as adsorbate, and the solid on which adsorption occurs is the adsorbent (Pontius, 1990). The process can occur at an interface between any two phases, as, liquid-liquid, gas liquid, gas-solid, or liquid-solid interfaces. In the adsorption process, the matter is extracted from one phase and concentrated at the surface of a second phase which is a surface phenomenon (Weber, 1972).

Surface reactions of this type must occur at least partly as a result of the forces active within the phase boundaries, or surface boundaries. Classical chemistry defines the properties of a system by the properties of its mass, for surface phenomena, however, the significant properties are those of the surface or boundary. Adsorption differs from absorption, which is the accumulation of substance in the interior of a non aqueous phase (Weber, 1972).

2.3.1. Types of Adsorption

Physical, chemical and exchange adsorption are the general types of adsorption. The basis distinction of these is the nature of the bonding between the molecule and the surface.

Physical adsorption is relatively nonspecific. It is caused by the operation of weak forces of attraction or van der Waals' forces between molecules. In this adsorption type, the adsorbed molecule is not affixed to a particular site on the solid surface, but is free to move about over the surface. The adsorbed material which is bound by the van der Waals' forces may condense and form several superimposed layers on the surface of the adsorbent. This type of adsorption is generally quite reversible.

The second type of adsorption is chemical adsorption. The forces acting on this kind of adsorption are much stronger than the ones acting on physical adsorption. The forces are comparable with those leading the formation of chemical compounds.

Normally the adsorbed material forms a layer over the surface which is only one molecule thick, and the molecules are not considered free to move from one surface site to another. When the surface is covered by the monomolecular layer, the capacity of the adsorbent is essentially exhausted. Chemical adsorption is seldom reversible. Generally the adsorbent must be heated to higher temperatures to remove the adsorbed materials. This type of adsorption is also called “chemisorption” or “activated adsorption”.

The adsorption characterized by electrical attraction between the adsorbate and the surface is called the exchange adsorption. In this type; ions of a substance concentrate at the surface as a result of electrostatic attraction to sites of opposite charge on the surface. In general, ions with greater charge, such as trivalent ions, are attracted more strongly toward a site of opposite charge than are ions with smaller charge, such as monovalent ions. Also, the smaller size of the ion gets (hydrated radius), the greater the attraction is.

Although there are significant differences among the three types of adsorption, there are instances in which it is difficult to assign a given adsorption to a single type. Many adsorption processes involving organic molecules result from specific interactions between identifiable structural elements of the sorbate and the sorbent. These interactions may be designated as “specific adsorption” as opposed to adsorption which occurs as a result of simple Coulombic interactions.

2.3.2. Adsorption Isotherms

One of the most important characteristics of an adsorbent is the quantity of adsorbate that it can accumulate. The constant temperature equilibrium relationship between the quantity of adsorbate per unit of adsorbent q_e and the equilibrium concentration of adsorbate in solution C_e is called the adsorption isotherm (Pontius, 1990).

2.3.2.1. Freundlich Isotherm. The Freundlich Isotherm is an empirical equation that describes much adsorption data. This equation has the form (Pontius, 1990):

$$q_e = K_f C_e^{1/n} \quad (2.1)$$

where;

q_e : mass of adsorbate adsorbed per unit mass of adsorbent

C_e : equilibrium concentration of adsorbate in solution

K_f and $1/n$: empirical constants

The parameters q_e and C_e are the equilibrium surface and solution concentrations, respectively. The constant K_f in the Freundlich equation is related primarily to the strength of adsorption. For fixed values of C_e and $1/n$, the larger the value of K_f , the larger the capacity q_e is. For fixed values of K_f and C_e , the smaller the value of $1/n$, the stronger the adsorption bond is. As $1/n$ becomes very small, the capacity tends to be independent of C_e , and the isotherm plot approaches the horizontal; the value of q_e then is essentially constant, and the isotherm is called irreversible. If the value of $1/n$ is large, the adsorption bond is weak (Pontius, 1990).

2.3.2.2. Langmuir Isotherm. Langmuir derived a relationship for q and C based on some assumptions that the energy of sorption for each molecule is the same and independent of surface coverage and maximum adsorption corresponds to a saturated monolayer of solute molecules on the adsorbent surface, that the energy of adsorption is constant, and that there is no transmigration of adsorbate in the plane of the surface. The Langmuir equation has the form:

$$q_e = \left[\frac{abC_e}{1 + bC_e} \right] \quad (2.2)$$

where;

q_e : mass of adsorbate adsorbed per unit mass of adsorbent

C_e : equilibrium concentration of adsorbate in solution

a, b : empirical constants

The constant a corresponds to the surface concentration at monolayer coverage and represents the maximum value of q_e that can be achieved as C_e is increased. The constant b is related to the energy of adsorption and increases as the strength of the adsorption bond increases (Pontius, 1990).

2.3.2.3. B.E.T. Equation. A different equation is more likely to describe adsorption where the adsorbate exceeds a monolayer. The Brunauer-Emmett-Teller (BET) model assumes that;

- Uniform energies of adsorption on the surface.
- A number of layers of adsorbate molecules form at the surface and that the Langmuir Equation applies to each layer.
- A given layer need not complete formation prior to initiation of subsequent layers; the equilibrium condition will therefore involve several types of surfaces (Weber, 1972).

2.3.3. Factors Influencing Adsorption

Adsorption is mainly affected by factors governing properties of both the adsorbate and the adsorbent (Weber, 1972).

2.3.3.1. Surface Area. Since the adsorption is a surface phenomenon, the extent of adsorption is proportional to specific surface area. Specific surface area can be defined as that portion of the total surface area that is available for adsorption. So that, the more finely divided and the more porous the solid, the greater is the amount of adsorption accomplished per unit weight of a solid adsorbent. Because the extent of a surface reaction will vary with available surface area, adsorption rate should exhibit a monotonic increase with some function of the inverse of the diameter of the adsorbent particles.

2.3.3.2. Nature of the Adsorbate. Chemical properties of the adsorbate gain importance in considering the nature of the adsorbate. These properties are:

Solubility of the Solute

The solubility of the solute is a controlling factor for adsorption equilibrium. In general, there is an inverse relationship between the extent of adsorption of a solute and its solubility in the solvent from which the adsorption occurs. As the solubility increases, the solute-solvent bond gets stronger, which results in a decrease in the extent of adsorption. In the case of an aqueous solution, the more hydrophilic, i.e. the more, substance likes water medium, the less it is adsorbed on solid. Conversely, a hydrophobic, water disliking, substance is adsorbed easily from aqueous solution. A substance may have the “solubility-amphoteric character” where its hydrophobic part is adsorbed at the surface, and the hydrophilic part is directed toward the aqueous phase.

Polarity of the Adsorbate

Solute polarity on adsorption is important. A polar solute prefers the phase which is more polar. In other words, a polar solute is strongly adsorbed from a non-polar adsorbent. But prefers a polar solvent to a non-polar adsorbent.

Dissociation Constant (pK_a) Value of the Adsorbate

Most of the weak acids or bases have pK_a and pK_b values respectively. Their ionization depends on the pH of the solution. A renowned relationship, the Henderson-Hasselbach equation states the connection between the pH of the medium, the pK value of a weak acid (or base) and the ratio of ionized to unionized forms:

$$pK = pH + \log (\text{unionized molecules/ionized particles})\dots\dots\dots(2.3)$$

From the known pH and pK_a (or pK_b) values; the anionic, cationic or neutral character of the adsorbent can be found out.

2.3.3.3. pH. Generally, adsorption increases at pH ranges where the species is neutral in charge. In addition, pH affects the charge on the surface, altering its ability to adsorb materials. Generally, adsorption of typical organic pollutants from water is increased with decreasing pH. In many cases this may result from neutralization of negative charges at the surface of the carbon with increasing hydrogen-ion concentration, thereby reducing hindrance to diffusion and making available more of the active surface of the carbon. This effect can be expected to vary in degree for different carbons, because the charges at the surfaces of the carbon depend on the composition of the raw materials and on the technique of activation.

2.3.3.4. Temperature. Adsorption reactions are normally exothermic; consequently the extent of adsorption generally increases with decreasing temperature. The enthalpy changes for adsorption are usually of the order of those for the condensation or crystallization reactions.

The change in the heat content of the system in which adsorption occurs, the total amount of heat evolved in the adsorption of a definite quantity of solute on an adsorbent, is termed the heat of adsorption, ΔH . Heats of gas-phase adsorption generally are several kcal per mole, but because water is desorbed from the surface when adsorption from aqueous solution occurs, heat effects for the latter process are somewhat smaller than those for gas-phase adsorption.

2.4. Nanoscale Particles and Nanotechnology

A nanometer is one-billionth of a meter. A sheet of paper is about 100,000 nanometers thick; a single gold atom is about a third of a nanometer in diameter. Dimensions between approximately 1 and 100 nanometers are known as the nanoscale. Unusual physical, chemical, and biological properties can emerge in materials at the nanoscale. These properties may differ in important ways from the properties of bulk materials and single atoms or molecules. Figure 2.1 illustrates the scale of objects in the nanometer range.

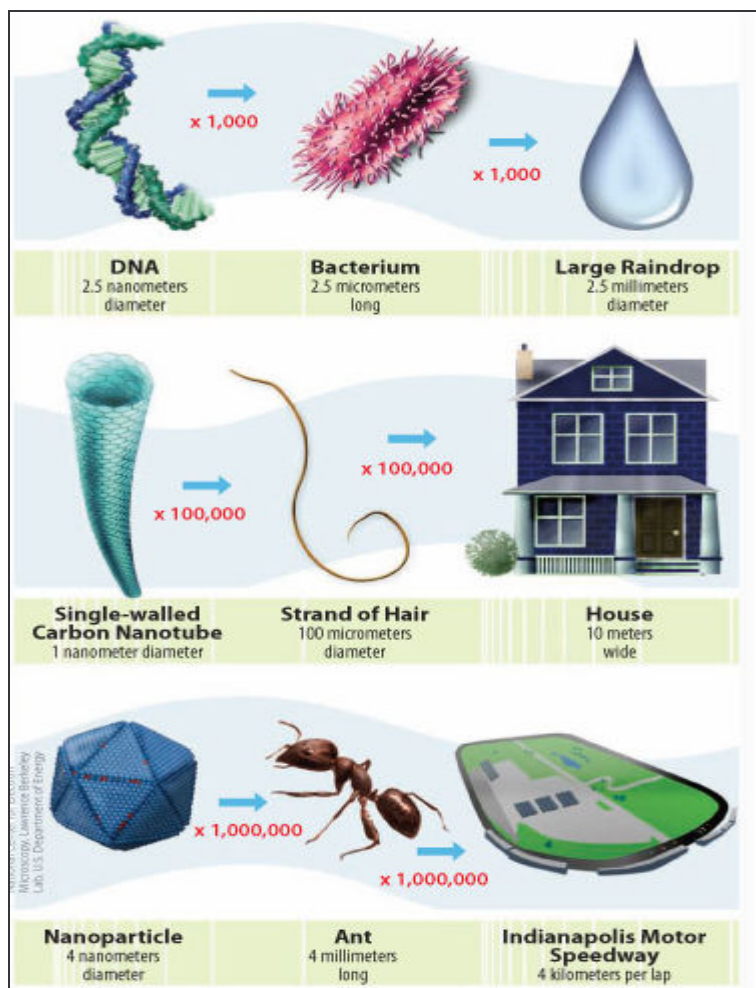


Figure 2.1 The scale of objects in the nanometer range (NNI website, courtesy of the National Centre for Electron Microscopy, Lawrence Berkeley Lab, US Department of Energy).

A nanoparticle is defined as a solid particle in the 1-1000 nm range that could be noncrystalline, an aggregate of crystallites, or a single crystallite (Klabunde, 1998). However, using nanoscale dimensions usually ranging from 1-100 nm is the target of nanotechnology. Nanoparticles are also named as “quantum dots”, due to their quantum mechanical properties and “nanocrystals” owing to the fact that the atoms within the particle are often highly ordered or crystalline (Holister et al., 2003).

The transition from microparticles to nanoparticles can lead to a number of changes in physical properties. Two of the major factors in this are the increase in the ratio of surface area to volume, and the size of the particle moving into the realm where quantum effects predominate. The increase in the surface area to volume ratio, which is a gradual progression as the particle gets smaller, leads to an increasing dominance of the behavior of atoms on the surface of a particle over that of those in the interior of the particle. This affects both the properties of the particle in isolation and its interaction with other materials (Holister et al., 2003).

The most important aspects while considering nanoparticles are synthesis, physical and chemical properties. But among these three, synthesis holds the first place. The nanoparticles of interest are almost always prepared in the laboratory as opposed to occurring naturally (Klabunde, 1998). There is a wide variety of techniques for producing nanoparticles. These essentially fall into three categories: condensation from a vapor, chemical synthesis, and solid state processes such as milling. Particles can then be coated for example with hydrophilic or hydrophobic substances, depending on the desired application (Holister et al., 2003).

Nanoparticles are currently made out of a very wide variety of materials, the most common of the new generation of nanoparticles being ceramics, which are best split into metal oxide ceramics, such as titanium, zinc, aluminum and iron oxides, to name a prominent few, and silicate nanoparticles generally in the form of nanoscale flakes of clay. The nanoparticles in metal and metal oxide nanopowders tend to be roughly the same size in all three dimensions, with dimensions ranging from two or three nanometers up to a few hundred (Holister et al., 2003).

2.4.1. The Fate of Nanoparticles in Water

Fate of nanomaterials in aqueous environments is controlled by aqueous solubility or dispersability, interactions between the nanomaterial and natural and anthropogenic chemicals in the system, and biological and abiotic processes. Waterborne nanoparticles generally settle more slowly than larger particles of the same material but can be removed from water by agglomeration or sorption and sedimentation.

Dispersed insoluble nanoparticles can be stabilized in water by interactions with naturally-occurring humic substances or other species. Biodegradation or association with biological materials may remove nanomaterials. Photo catalyzed reactions may alter the physical and chemical properties of nanomaterials and so alter their behaviour in water. Processes that control transport and removal of nanoparticles in water and wastewater are being studied to understand nanoparticle fate. Nanoparticle photochemistry is being studied with respect to its possible application in water treatment (Oberdorster et al., 2005).

Certain organic and metallic nanomaterials may possibly be transformed under anaerobic conditions, such as in aquatic (benthic) sediments. From past studies, it is known that several types of organic compounds are generally susceptible to reduction under such conditions. Complexation by natural organic materials such as humic colloids can facilitate reactions that transform metals in anaerobic sediments (Nurmi et al., 2005).

The fate of nano-sized particles in wastewater treatment plants is not well characterized. Wastewater may be subjected to many different types of treatment, including physical, chemical and biological processes, depending on the characteristics of the wastewater, whether the plant is a publicly owned treatment work (POTW) or onsite industrial facility, etc. Broadly speaking, nano-sized particles are most likely to be affected by sorption processes (for example in primary clarifiers) and chemical reaction. The ability of either of these processes to immobilize or destroy the particles will depend on the chemical and physical nature of the particle and the residence times in relevant compartments of the treatment plant. Sorption, agglomeration and mobility of mineral colloids are strongly affected by pH; thus pH is another variable that may affect sorption and settling of nanomaterials. Current research in this area includes the production of microbial granules that are claimed to remove nanoparticles from simulated wastewater (Ivanov et al., 2004).

Heterogeneous photoreactions on metal oxide surfaces are increasingly being used as a method for drinking water, wastewater and groundwater treatment. Semiconductors such as titanium dioxide and zinc oxide as nanomaterials have been shown to effectively catalyze both the reduction of halogenated chemicals and oxidation of various other pollutants, and heterogeneous photocatalysis has been used for water purification in treatment systems.

2.4.2. Nanoscale Particals' Use in Wet Remediation

The size and shape dependent optical and electronic properties of nanoparticles attracted many researchers to deploy them in the area of environmental remediation. Of particular interest is their application in advanced oxidation processes.

Nanoscale iron particles have been demonstrated to be very effective for the transformation and detoxification of a wide variety of common environmental contaminants, such as chlorinated organic solvents, organochlorine pesticides, and PCBs. Further investigations are underway with bimetallic nanoparticles (iron particles with Pt, Pd, Ag, Ni, Co or Cu deposits) and metals deposited on nanoscale support materials such as nanoscale carbon platelets and nanoscale polyacrylic acid (Zhang, 2003).

Metal remediation has also been proposed, using zero-valent iron and other classes of nanomaterials. Nanoparticles such as poly (amidoamine) dendrimers can serve as chelating agents, and can be further enhanced for ultrafiltration of a variety of metal ions (Cu (II), Ag(I), Fe(III), etc.) by attaching functional groups such as primary amines, carboxylates, and hydroxymates (EPA, 2007). Other materials such as silica-titania nanocomposites can be used for elemental mercury removal from vapors such as those coming from combustion sources, with silica serving in enhanced adsorption and titania used to photocatalytically oxidize elemental mercury to the less volatile mercuric oxide (EPA, 2007). Other research indicates that arsenite and arsenate may be precipitated in the subsurface using zero-valent iron, making arsenic less mobile (EPA, 2007). Finally, self-assembled monolayers on mesoporous supports (SAMMS) are nanoporous ceramic materials that have been developed to remove mercury or radionuclides from wastewater (EPA, 2007).

2.5. Ultrasound

Ultrasound is defined as any sounds of frequency above that to which human hear has no response (i.e., above 16 kHz). In practise, three ranges of frequencies are reported for three distinct uses of ultrasound (Mason and Cordemans, 1998): i) High frequency or diagnostic ultrasound (2-10 MHz); ii) Low frequency or conventional power ultrasound (20-100 kHz); and low-to-medium-frequency ultrasound (20-1000 kHz).

The use of power ultrasound has been well known for many years in fields such as medical, flow detections, emulsification, solvent degassing, cleaning; however chemical applications of ultrasound “sonochemistry”, in environmental processing is an emerging field. The chemical effects of ultrasound in liquids are largely linked to the formation of free radicals.

2.5.1. Ultrasonically-Induced Cavitation

Ultrasonic irradiation of liquids produces excessive energy for chemical reactions. This occurs because ultrasound causes other physical phenomena in liquids that create the conditions necessary to drive chemical reactions. The most important of these called “acoustic cavitation” consists of at least three distinct and successive stages: i) nucleation, ii) bubble growth, iii) implosive collapse (Suslick, 1990).

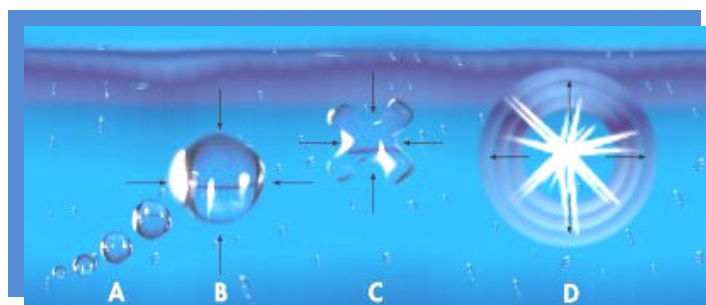


Figure 2.2. Formation, growth and implosion of a cavitation bubble (Suslick, 1994).

The first stage, also known, as “cavity formation” is a nucleated process, by which cavitation nuclei are generated from microbubbles trapped in micro crevices of suspended particles within the liquid (Suslick, 1990; Reisse, 1995). In the second stage, the bubbles grow and expand in a manner restricted by the intensity of the applied sound wave. With high-intensity ultrasound, a small cavity grows rapidly through inertial effects, whereas at lower intensities the growth occurs through “rectified diffusion”, proceeding in a much slower rate, and lasting many more acoustic cycles before expansion (Suslick, 1990). The third stage cavitation occurs only if the intensity of the ultrasound wave exceeds that of the “acoustic cavitation threshold” (typically a few watts/cm² for ordinary liquids exposed to 20 kHz) at this condition, the microbubbles overgrow to the extent where they can no longer efficiently absorb energy from the sound environment to sustain themselves, and implode violently, therefore, in a so called “catastrophic collapse” (Ince et al., 2001; Mason, 1990; Suslick et al., 1990).

There are two basic groups of theories advanced to explain energy-consuming chemical and physicochemical effects caused by cavitation, namely thermal and electrical. The thermal theories relate the presence of sonochemical effects to the appearance of a high temperature in a cavitation bubble during its adiabatic compression at a continuously growing velocity, while the electrical theories relate them to a discharge in a cavitation bubble because of the formation of electric charges on its walls (Margulis, 1995).

The second most accepted theory is “electrical theory” by Margulis (Margulis, 1995). This theory suggests that during bubble formation and collapse, enormous electrical field gradients are generated and these are sufficiently high to cause bond breakage and chemical activity.

The supercritical theory recently proposed by Hoffman and co-workers (Hua et al., 1997), suggests the existence of a layer in the bubble-solution interface where temperature and pressure may be beyond the critical conditions of water (647 K, 22.1 MPa) and showed that supercritical water is obtained during the collapse of cavitation bubbles generated sonolytically.

The plasma theory by Lepoint and Mullie (Lepoint and Mullie, 1994), also suggests extreme conditions associated with the fragmentative collapse is due to intense electrical fields and seems not to involve true implosion. They compared the origin of cavitation chemistry to corona-like discharge caused by a fragmentation process and supported and indicated the formation of microplasmas inside the bubble.

2.5.2. Possible Reaction Sites in the Cavitation Process

Experience in homogenous sonochemistry has shown that there are three potential sites for chemical reactions in ultrasonically irradiated liquids (Weavers et al., 1998; Suslick et al., 1986): (i) the cavitations bubble itself, (ii) the interfacial sheath between the gaseous bubble and the surrounding liquid, (iii) the surrounding liquid, the solution bulk as shown in Figure 2.3.

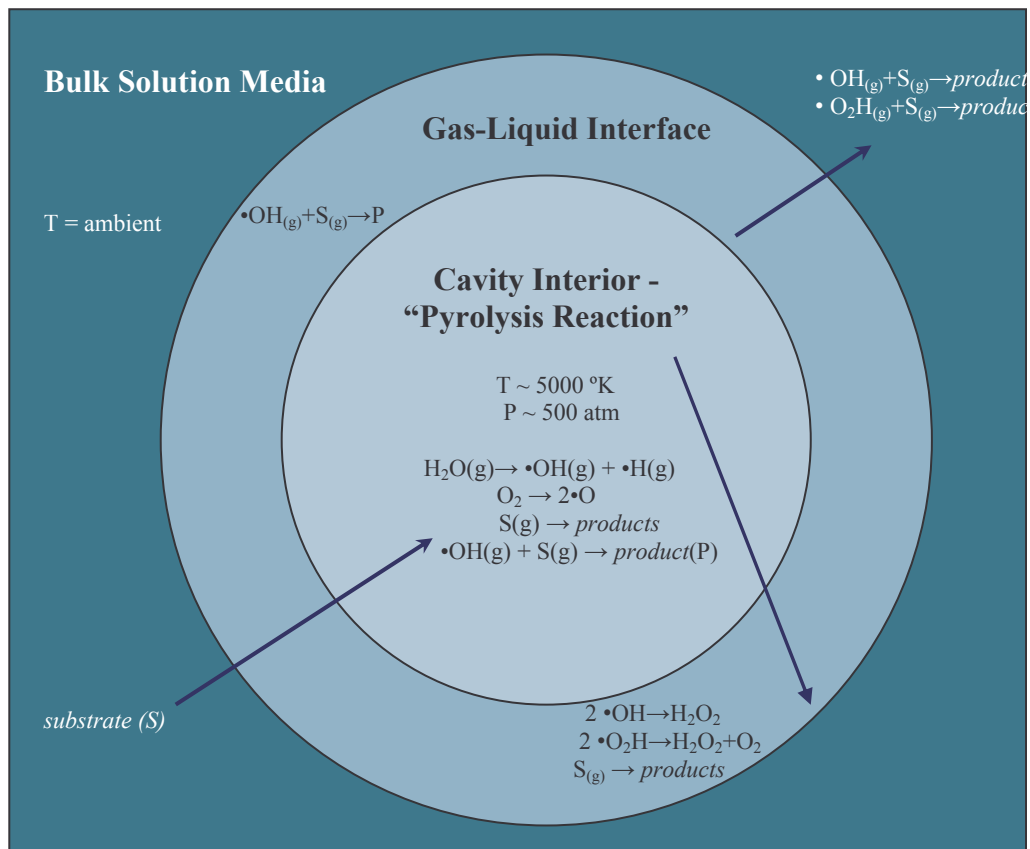


Figure 2.3. Possible sites of chemical reactions in homogeneous reaction media (Ince et al., 2001).

The hydroxyl radicals generated by water sonolysis may either react in the gas phase or recombine at the cooler gas-liquid interface and/or in the solution bulk to produce hydrogen peroxide and water as shown in the following equations (Ince et al., 2001; Riesz and Mason, 1991; Fischer et al., 1986):



If the solution is saturated with oxygen, peroxy and additional hydroxyl radicals are formed in the gas phase (due to the decomposition of molecular oxygen), and the recombination of the former at the cooler sites (interface or the solution bulk) produces more hydrogen peroxide, as shown (Ince et al., 2001; Makkino et al., 1982; Petriér et al., 1994):



2.5.3. Parameters Affecting Sonochemical Reaction Systems

Many parameters affect the sonochemistry of liquids, and it would seem that for almost the variable parameters which influence cavitation, there is an optimum value (Berlan and Mason, 1992).

2.5.3.1. Frequency. The more important cavity effects are reported to occur when the frequency of the wave is equal to the resonating frequency of the bubble. The resonance radius of a bubble excited by low frequency waves is reported to be ~170 μm (at 20 kHz), and the cavities entrapping such bubbles are said to be stable or long lived, with average life times of 10 μs (Mason, 1990; Petrier et al., 1994).

2.5.3.2. Properties of the Solute. The physicochemical properties of the contaminating species, such as vapour pressure (or Henry's constant), solubility and octanol-water partition coefficient can have dramatic effects on the cavitation collapse.

Hydrophobic chemicals with high vapour pressures have a strong tendency to diffuse onto the gaseous bubble interior, so that the most effective reaction site for their destruction is the bubble-liquid interface and/or the gaseous bubble itself (Kontronarou, et al., 1991; Drijivers et al., 1999). In contrast, hydrophilic compounds with low vapour pressure and low concentration tend to remain in the bulk liquid during irradiation, due to the repulsive forces exerted to-and-from the slightly hydrophobic bubble surfaces. The major reaction site for these chemicals, therefore, is the liquid medium, where they may be destroyed by oxidative degradation, provided that sufficient quantities of hydroxyl radicals are ejected into the solution during cavitation collapse (Ince et al., 2001; Drijivers et al., 1999).

2.5.3.3. Applied Pressure. Increased in the pressure of the system will give rise to a larger intensity of cavitation collapse and consequently an enhanced sonochemical effect (Mason, 1999). Too much pressure reduces the rate of reaction by decreasing the frequency or efficiency of bubble formations.

2.5.3.4. Properties of the Solvent. Cavities are more readily formed when using solvents with high vapour pressure, low viscosity, and low surface tension; however, the intensity of cavitations is benefited by using solvents of opposite characteristics. The intermolecular forces in the liquid must be overcome in order to form the bubbles. Thus, solvents with high densities, surface tensions, and viscosities generally have higher threshold for cavitations but more harsh conditions once cavitations begins (Young, 1989).

2.5.3.5. Solids as Catalysts. The addition of solid catalysts, such as glass beads, ceramic disks, SiO_2 , Al_2O_3 and talc into the reaction medium is another common method for enhancing cavitation effects. The presence of such material is reported to be especially useful for micronization of species (in ultrasonic cell disruption), and for the abrasion, activation and alteration of the chemical properties of catalyst surfaces during ultrasonic irradiation of liquid media (Mason and Cordemans, 1998).

2.5.3.6. Properties of Saturating Gas. Employing gases with large polytropic ratio values (γ) will enhance the adiabatic conditions in the collapsing bubble and improve sonochemical effects. For this reason monatomic gases (He, Ar, Ne) are used in preference to diatomic gases (N_2 , air, O_2). However it must be remembered that this dependence on γ is a simplistic view, since the sonochemical effects also depend on the thermal conductivity of the gas, even if a strict relationship between the properties of gases and the sonochemical effect has not been observed.

Both cavitation threshold and the intensity of the shockwave released on the collapse of the bubble decrease when the gas content of a liquid increases (Mason and Lorimer, 2002).

2.5.3.7. Power Intensity. In general an increase in the intensity will provide for an increase in the sonochemical effects. Cavitation bubbles, initially difficult to create at higher frequencies (due to the shorter time periods involved in the rarefaction cycle) will now be possible, and since both collapse time and the temperature and

the pressure on the collapse are dependent on the pressure in the liquid at the time of collapse, bubble collapse will be more violent. However, it must be realised that intensity cannot be increased indefinitely, since the maximum bubble size is also dependent upon the pressure amplitude (Mason and Lorimer; 2002).

2.5.3.8. Temperature. Lowering the bulk solution temperature has been shown to actually increase the effect of sonication. This is due to a decrease in the vapour pressure of the solvent, which leads to an increase in the intensity of the bubble. At low vapor pressure, less vapour has an opportunity to diffuse into the bubble which favors the more violent collapse. Also, as liquid temperature decreases, the amount of gas dissolved increases and the vapor pressure of the liquid decreases. Very volatile solvents lead to relatively high pressures in the bubble and also cushion the collapse (Adewuyi, 2001).

2.5.4. Application of Ultrasound in Decontaminating Tannery Wastewater.

There are several reliable methods for simple chromium ion removal, including chemical precipitation, adsorption and ion exchange. Precipitation is a simple and effective process, but it is not applicable for removal of complex chromium ion (Zhao et al., 2004). Ion exchange can effectively remove chromium ions, but it is not practical and ion-exchange resin can be used in a very limited pH range only. Adsorption is well known for the effectiveness in removing heavy metal pollutants, but the adsorption capacities must be boosted by modification of adsorbent with suitable chemicals (Zhao et al., 2004). Treating wastewaters of this type are still in the phase of investigation, with number of problems to be solved.

In studies reported in the literature on such alternate solutions, it is found that in general only one pollution component (mainly chromium) is considered, so that much research is required for practicality of these solutions. Regarding the use of ultrasound in decontaminating tannery wastewater, the literature reports only one study, in which short frequency ultrasound was found to enhance sedimentation of sludge that forms in conventional plants as a result of Cr(III) precipitation with NaOH (Guo et al., 2006).

3. MATERIALS AND METHODS

3.1. Materials

3.1.1. Chemicals Used in the Experiments

Adsorbate

Chromium (III): $\text{CrK}_2\text{O}_8 \cdot 12\text{H}_2\text{O}$ (98.5 % pure, as solid) was obtained from Fluka.

Glucose: Glucose D(+) monohydrate was obtained from Carlo Erba.

Pluck: Pluck which has a 14.000 mg L^{-1} COD purchased from a restaurant.

Adsorbent

Microparticle in powder form and nanoparticle in suspension form were used in silent and sonicated adsorption systems. The particles used in these experiments are listed below:

- H-200 Zero Valent Iron (Hepure, USA) was used as in powder form:
- Reactive Nanoscale Iron Particles (RNIP) (Toda Kogyo Corp, Japan).was used in suspension form.

Sodium Hydroxide and Hydrochloric Acid

Analytical grade sodium hydroxide (NaOH) and hydrochloric acid (HCl) at various concentrations used for pH adjustment were obtained from Merck.

Membrane Filter Paper

0.45 μm Schleicher & Schuell filter papers obtained from Interlab were used for the filtration of test solutions and for removing the turbidity of residual adsorbent before atomic absorption spectrometer analysis.

3.1.2. Experimental Setup

3.1.2.1. Horizontal Shaker. The adsorption experiments of chromium on microparticle and nanoparticle were performed in 250 mL erlenmeyer flasks shaken at 100 RPM and 25 °C. A Memmert SV 1422 horizontal shaker was used in all experiments. Adsorption isotherms were determined using the equilibrium data obtained with different concentrations of adsorbents contacted with 10 mg L⁻¹ of chromium. A photograph of the shaker is presented in Figure 3.1.



Figure 3.1. Photograph of horizontal shaker

3.1.2.2. Sonication Experiments (20 kHz probe inserted reactor). The system consists of a 100 mL glass cell surrounded by a water-cooling jacket to keep the reactor at constant temperature (25 ± 0.5 °C); a Bandelin sonoplus HD2200 a probe type transducer (probe tip area = 1.13 cm²), emitting ultrasonic waves at 20 kHz and a 180 W generator. The horn was submerged 3 cm from the top of a reaction cell, which had an effective volume of 80 mL. The system was mounted in a polyurethane isolating material to prevent excessive noise. A photograph of the reactor is presented in Figure 3.2.

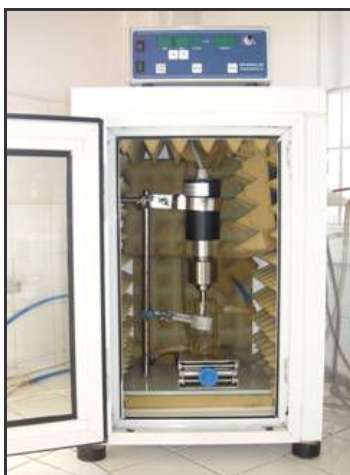


Figure 3.2. Photograph of 20 kHz probe inserted reactor

3.2. Methods

3.2.1. Preparation of the Test Solutions.

Single Solution : Stock chromium (III) solutions of 10 mg L^{-1} were prepared by dissolving the $\text{CrK}_2\text{O}_8 \cdot 12\text{H}_2\text{O}$ in deionized water.

Solution Matrix 1: Solution matrix 1 was prepared by inserting glucose into the stock chromium solution of 10 mg L^{-1} as organic matter to achieve 100 and 200 mg L^{-1} BOD_5

Solution Matrix 2: 500 g of pluck was boiled in water and allowed to cook and dissociate for 1 hour. The pluck solution was diluted to 1000 mg L^{-1} as COD followed by adding 0.38 g of $\text{CrK}_2\text{O}_8 \cdot 12\text{H}_2\text{O}$ to have a Cr^{3+} concentration of 40 mg L^{-1}

Water used for the preparation of the all solutions and dilution of the samples was produced from deionized water using a Millipore Milli-Q gradient apparatus.

3.2.2. Adsorption Experiments

For the determination of adsorbability of the iron particles, adsorption experiments were carried out in 250 mL flasks shaken at 100 RPM and $25 \text{ }^\circ\text{C}$ in the Memmert SV 1422 horizontal shaker. The effective solution volume was 100 ml at all times. Different concentrations of adsorbents were contacted with fixed chromium concentration. Initial and final concentrations of the chromium in adsorption flasks were measured. The effect of pH, contact time and initial adsorbent concentration were analyzed. To evaluate the rate of sorption, samples were withdrawn from the reactor at different times for the atomic absorption spectrometer analysis. The samples were first filtered through $0.45 \text{ }\mu\text{m}$ membrane filters before the analysis

3.2.3. Sonication Experiments

The combinative effect of ultrasound coupled with microparticle and nanoparticle on the removal of chromium was tested by sonicating the test solutions in the presence of these particles at various concentrations. The effect of pH, sonication duration and initial adsorbent concentration were analyzed. Samples were withdrawn from the reactor at different times for the atomic absorption spectrometer analysis. The samples were first filtered through 0.45 μm membrane filters before the analysis.

3.3. Analytical Equipment

Sartorius Balance was used for weighing, potassium chromium sulphate, reactive nanoscale iron particles and H-200 zero-valent iron.

Perkin Elmer Optima 2100 Atomic Absorption Spectrometry was used for the determination of the residual chromium concentration in samples taken from adsorption and ultrasound experiments. The instrument was calibrated by standard solutions of chromium (III) and the absorbance of chromium was measured at a wavelength of 357.9 nm.



Figure 3.3. Photograph of atomic absorption spectrometry

Chemical oxygen demand was monitored by using Hach Lange DR2010 model spectrophotometer. The instrument was calibrated by standard solutions of potassium hydrogen phosphate (KHP) and COD was measured at a wavelength of 600 nm.



Figure 3.4. Photograph of spectrophotometer

Biochemical oxygen demand was evaluated by using WWT OXI 330 model oxygen meter.

4. RESULTS AND DISCUSSION

4.1. Adsorption of Chromium on Reactive Nanoscale Iron Particles (RNIP)

In this part of the study, the adsorption capacity of chromium (III) on RNIP was investigated. Specifically, the purpose was to determine the impact of various operating parameters on the adsorption of chromium and selection of the best fit isotherm. The effect of adsorbent concentration was studied by evaluating the chromium (III) concentration left in water at different adsorbent concentrations. The impact of pH on the adsorption capacity was assessed by monitoring the residual chromium at pH 3, 4 and 5. The adsorption isotherms were constructed by contacting different concentrations of RNIP with a fixed concentration of chromium (10 mg L^{-1}). In the following sections the term “chromium” refers to Cr(III).

All adsorption runs were carried out in 250 mL flasks shaken at 100 RPM and $25 \text{ }^{\circ}\text{C}$ Memmert SV 1422 horizontal shaker was used throughout the experiments.

4.1.1. Effect of Adsorbent Concentration

To determine the effect of adsorbent concentration on the adsorption of chromium, the residual concentration of chromium was monitored at concentration ranges 10, 15, 20, 25 and 30 g L^{-1} of RNIP during 4 hour. The optimum RNIP concentration was found by investigating the adsorption equilibrium upon increased adsorbent concentrations as shown in Figure 4.1.

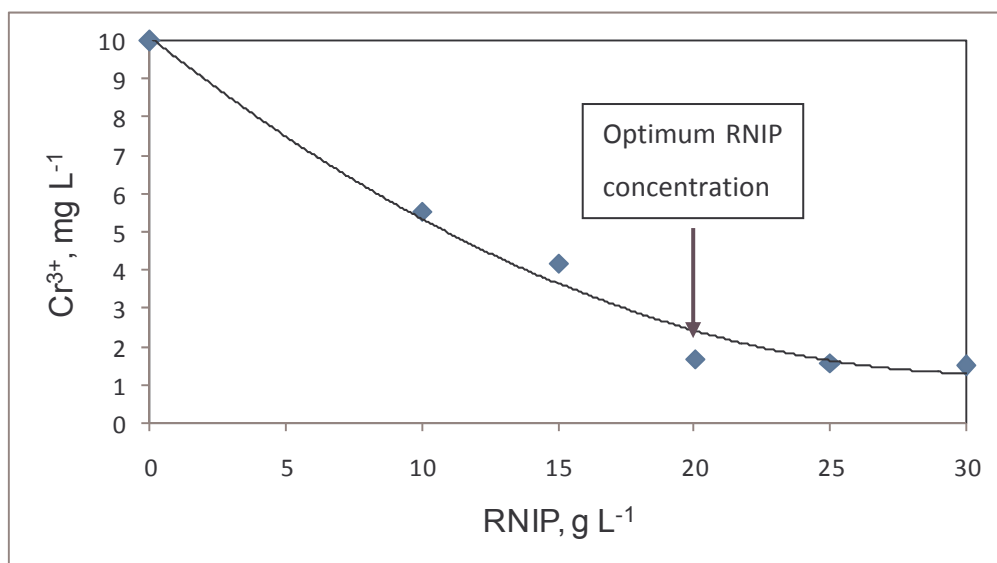


Figure 4.1. Determination of optimum RNIP concentration.

It was obvious that the residual concentration of chromium decreases until the concentration of 20 g L⁻¹ was reached. After that point, the fraction of Cr(III) removal did not change too much with increasing concentrations of RNIP as shown in Figure 4.2.

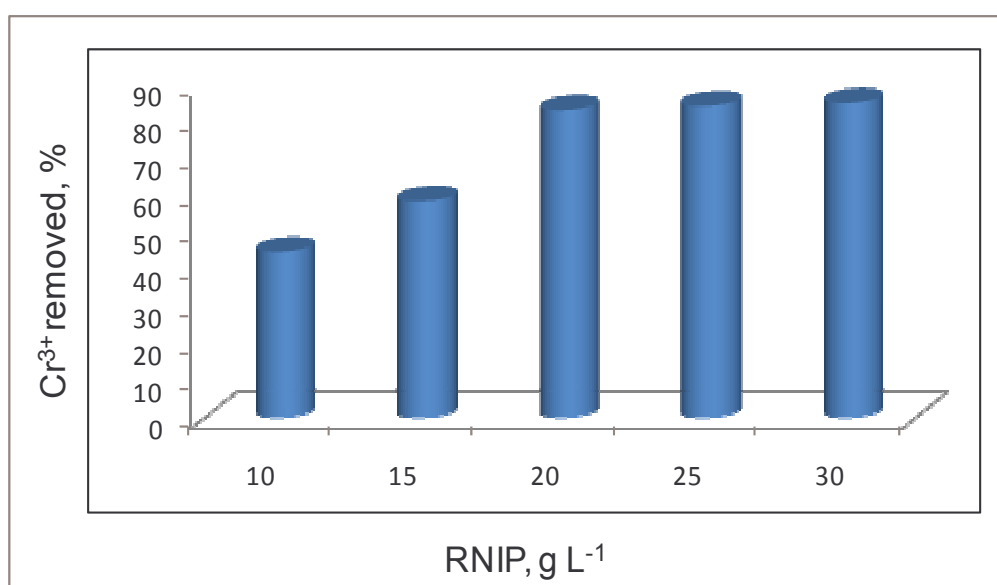


Figure 4.2. Effect of RNIP concentration on the fraction of Cr(III) removal.

4.1.2. Selection of the Isotherms

The adsorption isotherms were constructed by contacting different concentrations of RNIP (10 to 30 g L⁻¹) with a fixed concentration of chromium (10 mg L⁻¹). Samples were collected periodically to monitor the reduction in chromium concentration. The data were evaluated by fitting them into the linearized forms of Freundlich and Langmuir Equations, defined in Chapter 2 as Equation 2.1 and 2.2, respectively.

The constant K_f in the Freundlich isotherm is related primarily to the strength of adsorption. For fixed values of C_e and $1/n$, the larger the value of K_f , the larger the capacity q_e is. For fixed values of K_f and C_e , the smaller the value of $1/n$, the stronger the adsorption bond is.

In the Langmuir isotherm, the constant corresponds to the surface concentration at monolayer coverage and represent the value of q_e , that can be achieved as C_e is increased. The constant b is related to the energy of adsorption and increases as the strength of the adsorption bond increases (Pontius, 1990).

The adsorption experiments revealed that when chromium was contacted with RNIP, adsorption was observed. Adsorption isotherms constructed for RNIP are illustrated in Figures 4.3.a and 4.3.b. It can be seen that data obtained from RNIP fit both to the Langmuir isotherm and Freundlich isotherm.

Freundlich Isotherm

The values of K_f and $1/n$ were determined from a plot of $\ln q_e$ versus $\ln C_e$ where $\ln K_f$ is the intercept and $1/n$ is the slope of the predicted straight line. Figure 4.3.a. illustrates the determination of Freundlich constants for 10 mg L^{-1} Cr(III) exposed to various RNIP concentration at pH 5 for 180 minutes.

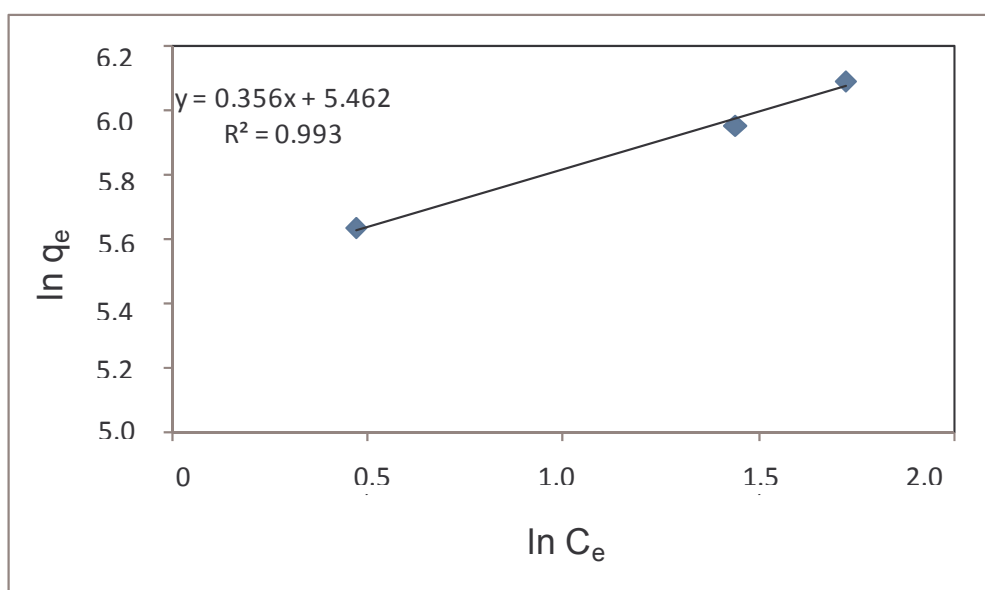


Figure 4.3.a. Adsorption of Cr(III) on RNIP and the linearized best fit Freundlich Isotherm.

Langmuir Isotherm

The values of Langmuir constants a and b were determined from a plot of $1/q_e$ versus $1/C_e$ where $1/b$ is the intercept and $1/ab$ is the slope of the predicted straight line. $1/ab$ and $1/b$ are the indicators of the adsorption capacity and the adsorption intensity, respectively. Results are presented in Figure 4.3.b.

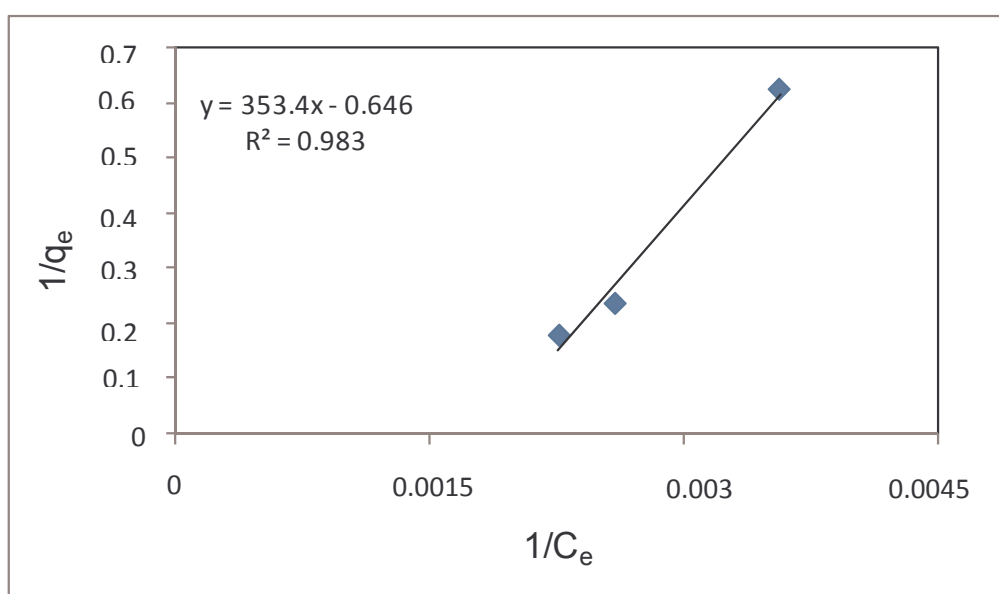


Figure 4.3.b. Adsorption of Cr(III) on RNIP and the linearized best fit Langmuir Isotherm.

Empirical constants of Freundlich and Langmuir equations for chromium are presented in Table 4.1.

Table 4.1. Freundlich and Langmuir constants for chromium in the presence of RNIP.

Freundlich		Langmuir	
$1/n$	K_f	a	b
0.356	235.5	1.548	0.00018

4.1.3. Effect of Contact Time

The changes in the chromium concentration were monitored during 4 hours to follow the effect of contact time on the chromium removal. The contact time required for 82 per cent removal by RNIP adsorption was found as 3 hours by inspection of the fraction of chromium removal as shown in Figure 4.4.

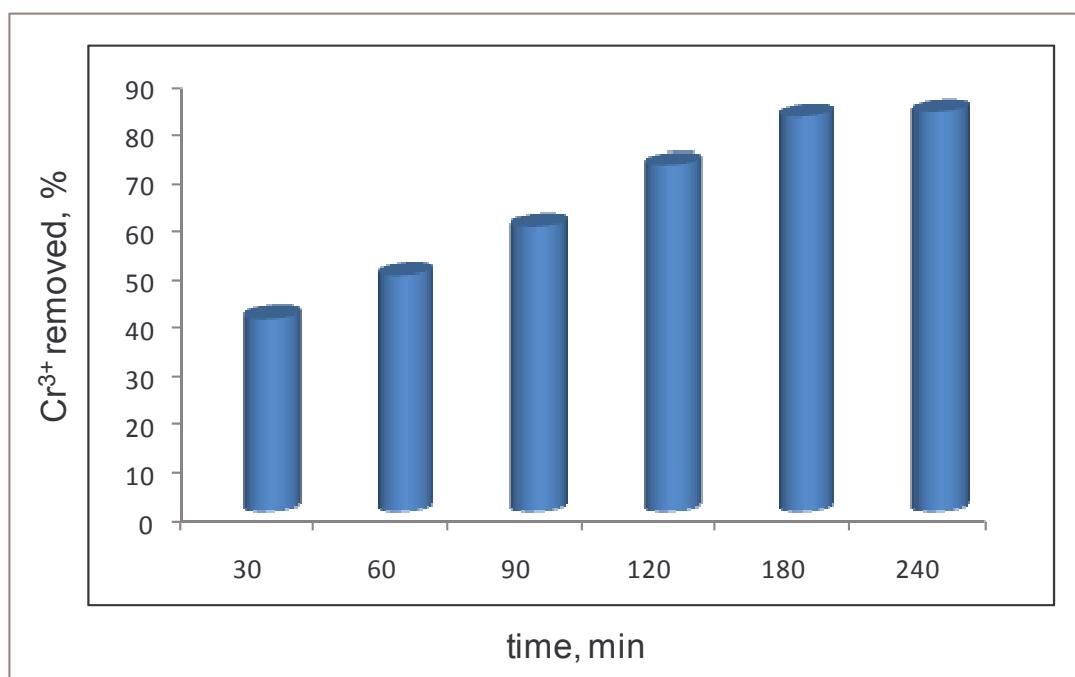


Figure 4.4. Optimization of contact time for Cr(III) adsorption on RNIP.

4.1.4. Effect of pH

The effect of pH was investigated by adsorption of chromium at pH 3, 4 and 5 during 3 hour. Effect of pH on adsorption of chromium on RNIP is presented in Figure 4.5.

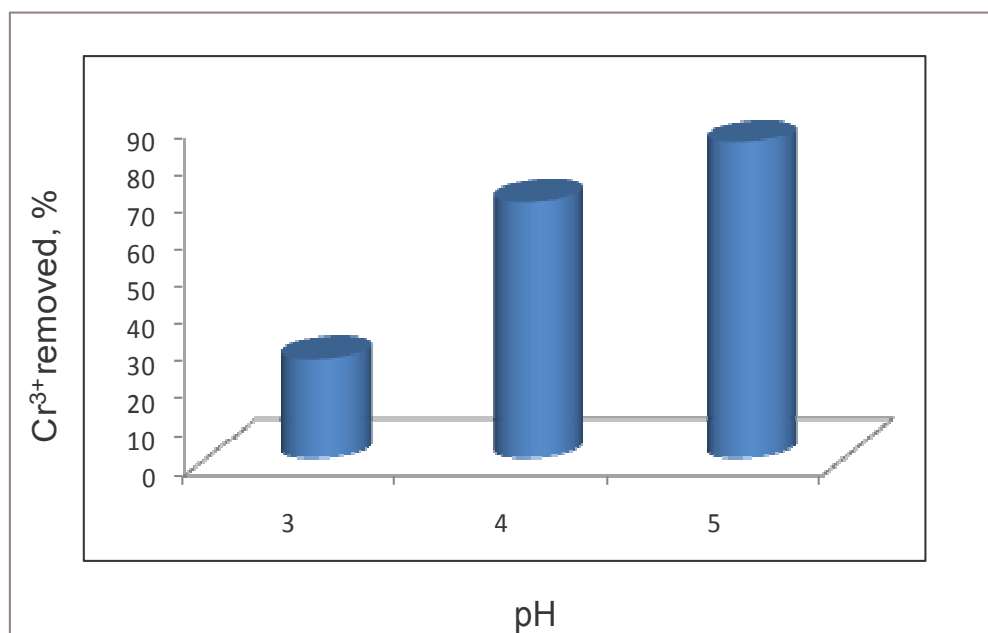


Figure 4.5. Effect of pH on the adsorption of chromium on RNIP.

It was found that effectiveness of RNIP for the adsorption of Cr(III) increases with an increase in pH. The removal efficiency at pH 5 is greater than that for pH 3 and 4. Therefore, pH 5 was selected as the working pH.

According to the speciation diagram of chromium shown in Figure 4.6 the predominant species below pH 2 is Cr(III) and between pH 6.5 and 10 the predominant species is Cr(OH)₃. Between pH values of 3 and 5, Cr(III) adsorbed as Cr(OH)²⁺ and Cr₃(OH)₄⁵⁺.

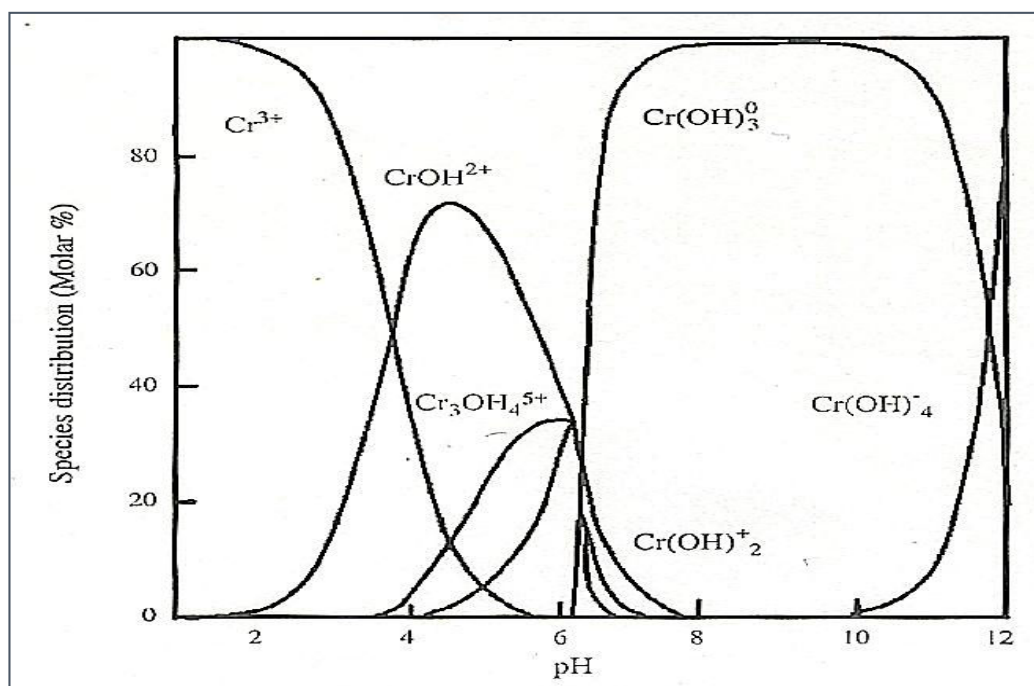


Figure 4.6. Speciation diagram for Cr(III) complexes present in aqueous solution.

4.1.5. The Rate of Chromium Removal

The rate of chromium removal was found to follow one phase exponential decay in accordance with Equation 4.1. The difference of this equation from the classical pseudo-first order rate explanation is the parameter P, which is almost zero in the classical equation.

$$C = C_0 e^{-kt} + P \text{ (Plateau)} \quad (4.1)$$

Where;

C: concentration of chromium at time = t, mg L⁻¹

C₀: concentration of chromium at time = 0, mg L⁻¹

k: first order decay rate constant, s⁻¹

t: time, s

Normalized plots of Cr^{3+} against time and the estimated degradation rate constants of chromium are presented in Figures 4.7. Estimated decay rate coefficients for chromium are presented in Table 4.2.

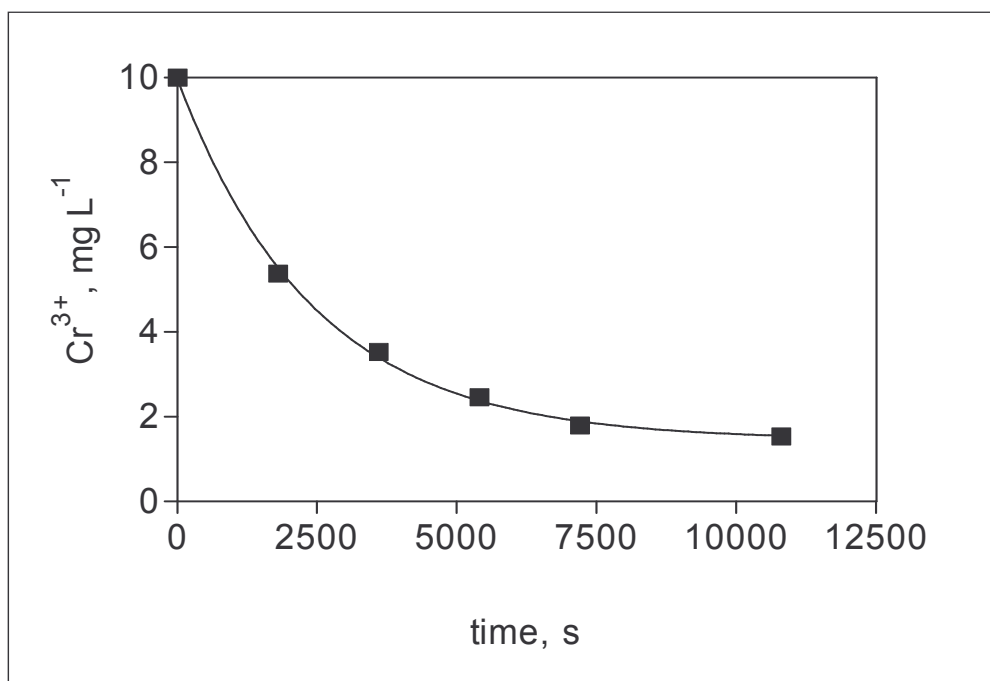


Figure 4.7. Estimation of the decay rate coefficients for chromium (pH: 5 RNIP: 20 mg L⁻¹).

Table 4.2 Chromium removal rate constant and the related statistical parameters (in the presence of RNIP).

k (s⁻¹)	R²	P	Half-life
4.10 10 ⁻⁴ ± 2.06 10 ⁻⁵	0.998	1.451 ± 0.12	1.689 ± 88.26

4.2. Adsorption of Chromium on H-200 Zero Valent Iron

In this section, the adsorption capacity of chromium (III) on H-200 zero-valent iron was investigated. Specifically, the purpose was to determine the impact of various operating parameters on the adsorption of chromium and selection of the best fit isotherm. The effect of adsorbent concentration was studied by evaluating the chromium (III) concentration left in water at different adsorbent concentrations. The impact of pH on the adsorption capacity was assessed by monitoring the residual chromium at pH 3, 4 and 5. The adsorption isotherms were constructed by contacting different concentrations of H-200 zero-valent iron with a fixed concentration of chromium (10 mg L^{-1}). In the following sections the term “chromium” refers to Cr(III) and the term “ZVI” refers to H-200 zero-valent iron.

All adsorption runs were carried out in 250 mL flasks shaken at 100 RPM and 25 °C Memmert SV 1422 horizontal shaker was used throughout the experiments.

4.2.1. Effect of Adsorbent Concentration

The effect of adsorbent concentration on the adsorption of Cr(III) was studied by evaluating the Cr(III) concentration left in water at concentration ranges 0.1, 0.2, 0.4, 0.6, 0.7 and 0.8 g L^{-1} of ZVI. The optimum adsorbent concentration was found by investigating the adsorption equilibrium upon increased adsorbent concentrations as shown in Figure 4.8.

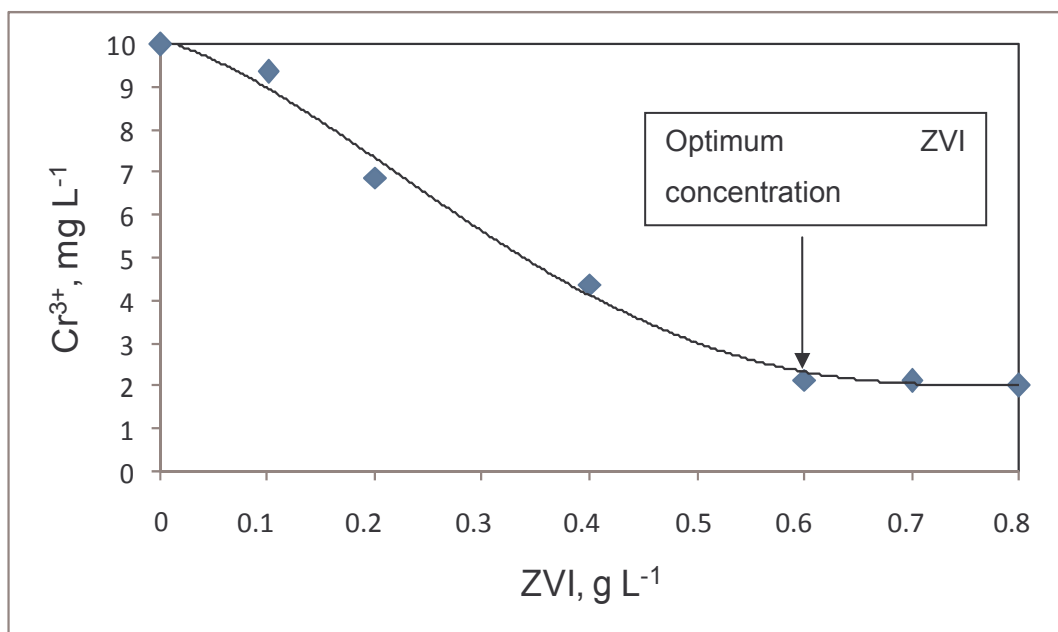


Figure 4.8. Determination of optimum ZVI concentration.

0.6 g L^{-1} ZVI was found as optimum adsorbent concentration. After that point, the fraction of chromium removal did not change very much with increasing concentrations of adsorbent as shown in Figure 4.9.

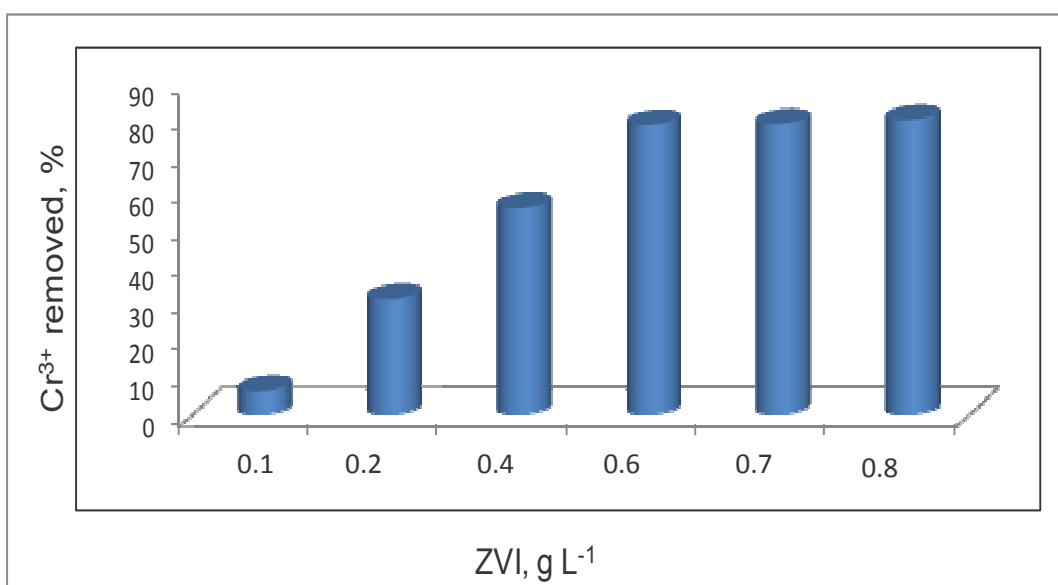


Figure 4.9. Effect of ZVI concentration on the fraction of chromium removal.

4.2.2. Selection of the Isotherms

The adsorption isotherms were constructed by contacting different concentration of ZVI (0.1, 0.2, 0.4, 0.6, 0.7 and 0.8 g L⁻¹) with a fixed concentration of chromium (10 mg L⁻¹) Samples were collected periodically to monitor the reduction in chromium concentration.

Figure 4.10.a. and Figure 4.10.b illustrates the determination of Freundlich and Langmuir constants for chromium (10 mg L⁻¹) exposed to various ZVI concentrations at pH 4 for 120 minutes, respectively.

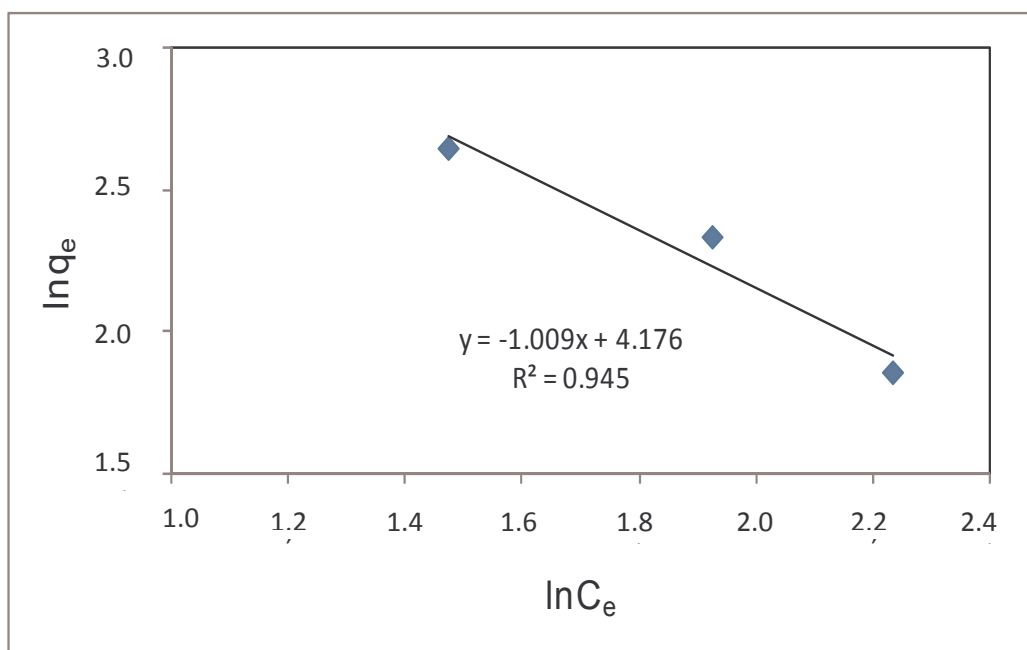


Figure 4.10.a. Adsorption of chromium on ZVI and the linearized best fit Freundlich isotherm.

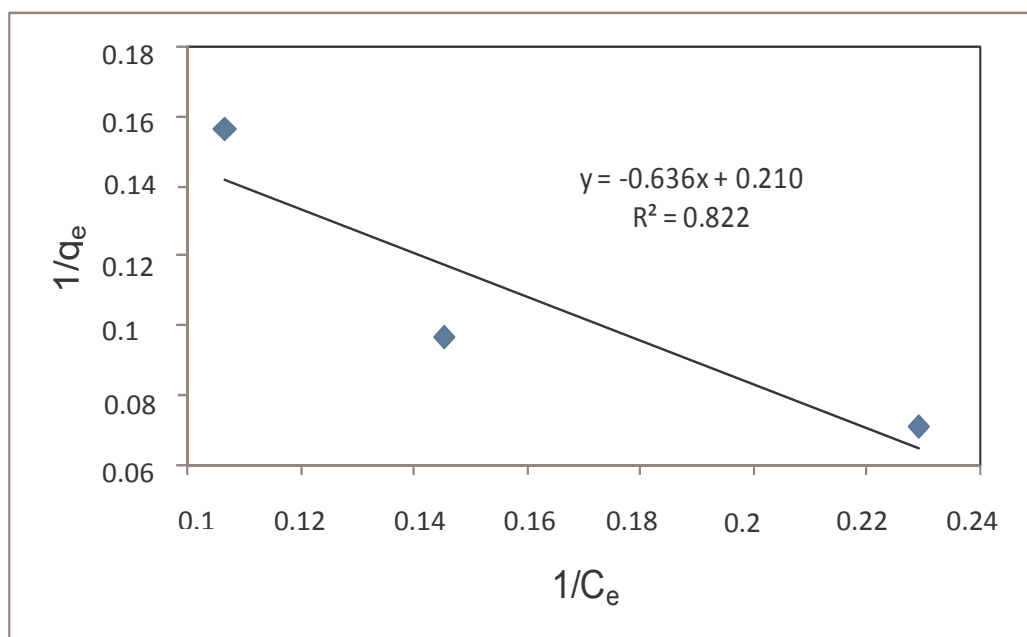


Figure 4.10.b. Adsorption of chromium on ZVI and the linearized best fit Langmuir isotherm.

When chromium was contacted with RNIP or ZVI, adsorption was observed. Adsorption isotherms constructed for RNIP and ZVI show that the Freundlich Isotherm represents the data more precisely.

Empirical constants of Freundlich and Langmuir equations for chromium are presented in Table 4.3.

Table 4.3. Freundlich and Langmuir constants for chromium in the presence of ZVI.

Freundlich		Langmuir	
$1/n$	K_f	a	b
-1.009	65.10	-0.33	4.762

4.2.3 Effect of Contact Time

At the end of 120 minutes, 79 per cent of chromium removal was gained. After that point, the removal efficiency reached equilibrium. The equilibrium curve is shown in Figure 4.11.

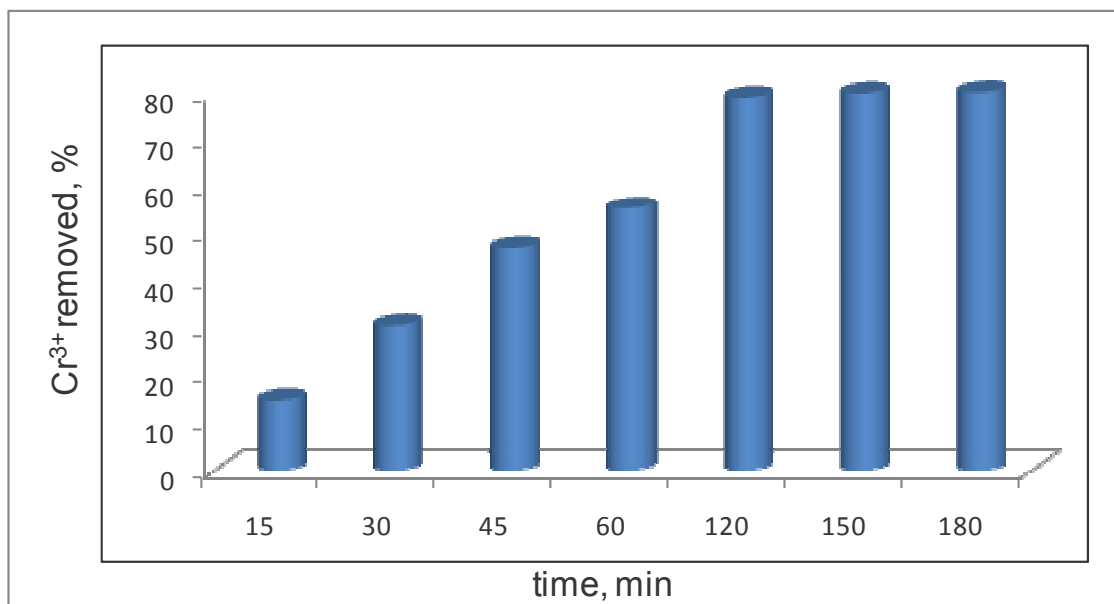


Figure 4.11. Optimization of contact time for Cr(III) adsorption on ZVI.

4.2.4. Effect of pH

The effect of pH was investigated by adsorption of chromium at pH 3, 4 and 5. Effect of pH on adsorption of chromium on ZVI is presented in Figure 4.12.

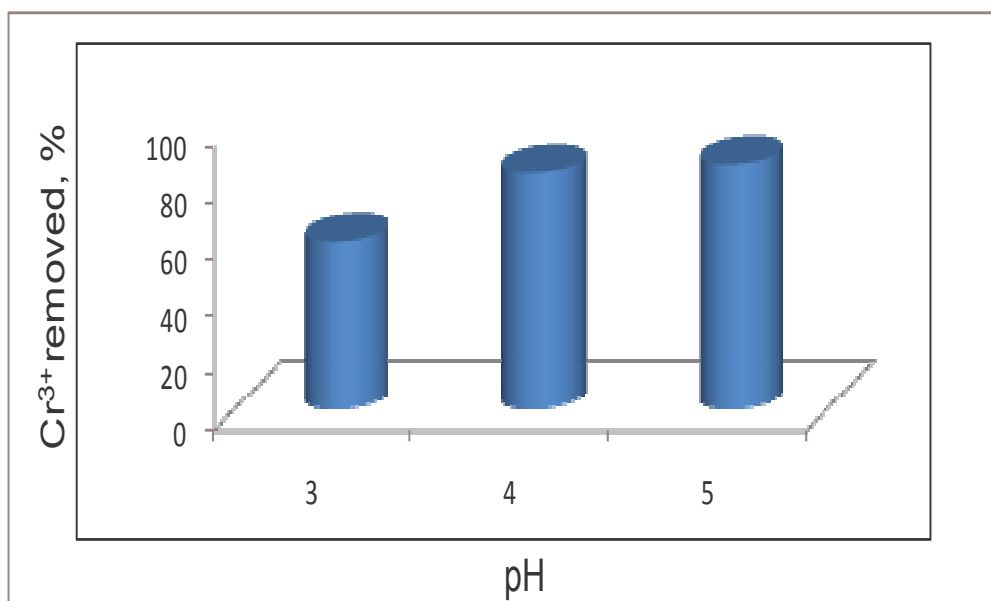


Figure 4.12. Effect of pH on adsorption of chromium on ZVI.

It was found that the adsorption of chromium on ZVI is better at pH 4 and 5 than pH 3 and there is no more difference between the removal efficiency at pH 4 and 5. As a result, the working pH was chosen as 4 since the effluents formed after chromium tanning has a pH usually as 4.

The optimum pH was found 5 for both adsorbents in silent and sonicated systems. Yet; the fraction of chromium removal in the presence of ZVI was nearly same at pH=4 and pH=5.

4.2.5. The Rate of Chromium Removal

The rate of chromium removal was found to follow one phase exponential decay in accordance with Equation 4.1. Normalized plots of Cr^{3+} against time and the estimated decay rate constants of chromium are presented in Figures 4.7 and Table 4.4, respectively.

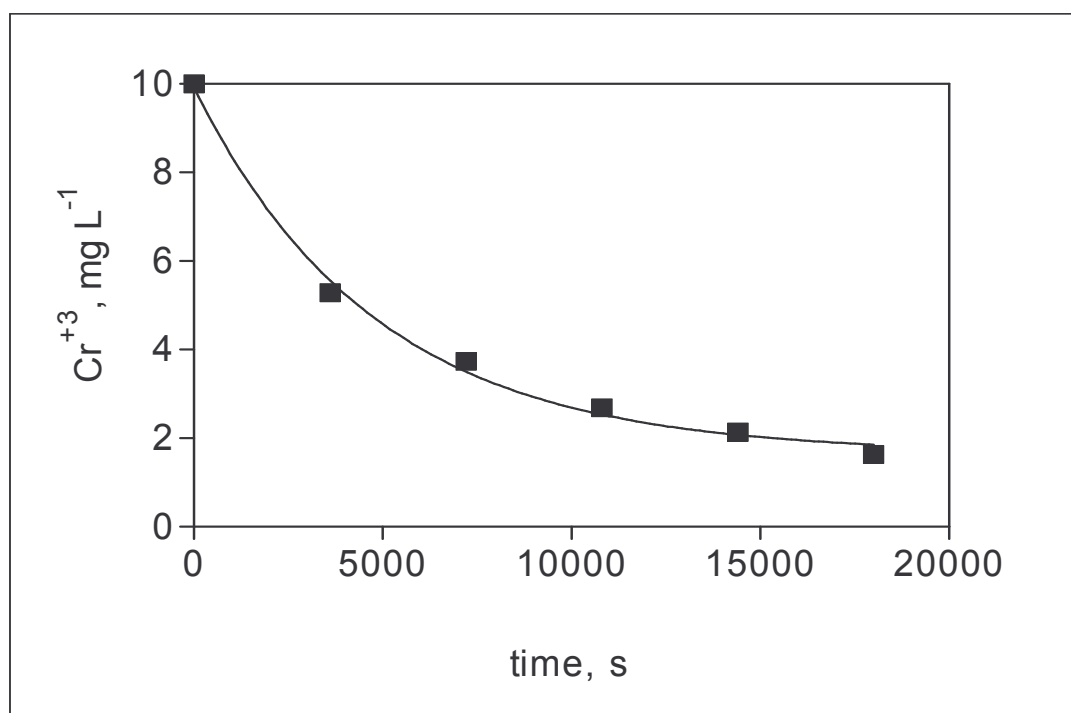


Figure 4.13. Estimation of the decay rate coefficients for chromium (pH: 4 ZVI: 0.6 mg L⁻¹).

Table 4.4 Chromium removal rate constant and the related statistical parameters (in the presence of ZVI).

k (s⁻¹)	R²	P	Halflife
2.08 10 ⁻⁴ ±2.69 10 ⁻⁵	0.996	1.662 ± 0.25	3328 ± 856

The degradation of chromium by adsorption in the presence of RNIP and ZVI followed first order decay kinetics with stabilization of the concentration at a constant value called the Plateau.

4.2.6. Effect of Solution Matrix 1

The effect of solution matrix 1 was investigated by adding organic matter as glucose to a chromium solution of 10 mg L^{-1} and running the adsorption experiments with ZVI at pH 4 for 6 hours. Organic matter was inserted into solution as glucose, as explained in Section 3. Fractions of chromium and BOD_5 removal are presented in Figures 4.14.

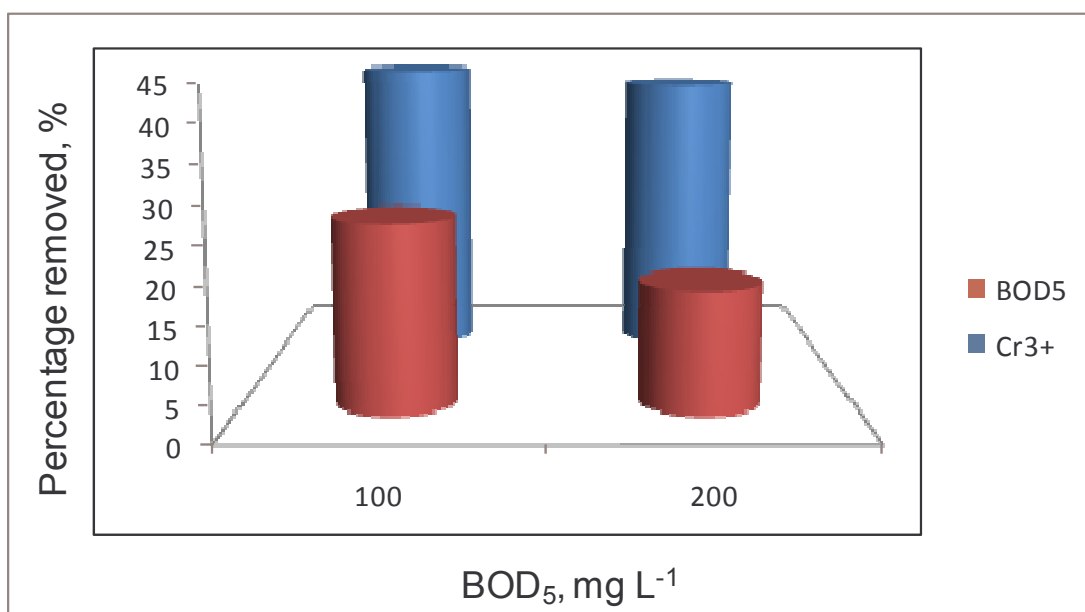


Figure 4.14. Fractions of chromium and BOD_5 removal by adsorption in the presence of ZVI (pH:4, time: 2 hour).

It was found that the fraction of chromium removal for the single solution is greater than that of mixtures. Therefore, the fraction of chromium removal is approximately equal while BOD_5 is 100 mg L^{-1} and 200 mg L^{-1} .

It was found that as the initial concentration of BOD_5 was increased, the fraction of BOD_5 removal decreased. Total BOD_5 removal in each mixture after 6 hour exposure to ZVI was 59% and 51%, respectively.

4.3. Ultrasound and Nanoparticles

As discussed in Chapter 2, the effect of low frequency ultrasound in heterogeneous solution is to improve surface purification and to reduce surface areas. Accordingly, adsorption experiments were repeated with 20 kHz ultrasonic irradiation to observe the enhancement in adsorption of chromium. The role of operating parameters on the rate of chromium adsorption was studied. A summary of the operating parameters considered is presented in Table 4.5. Ultrasonic irradiation was employed in. The impact of pH on the removal of chromium was assessed by monitoring the residual chromium at pH 3, 4 and 5. To determine the effect of contact time the residual concentration of chromium was evaluated every ten minutes.

RNIP and ZVI were used as adsorbents. Test samples were prepared from the stock using ultra-pure milli-Q water. Samples were withdrawn from the reactor for Atomic Absorption Spectrometer analysis.

Table 4.5. Operating parameters considered in the application of sonication to chromium.

Operating Conditions	Value
Frequency	20 kHz
pH	3, 4, 5
Contact time	10, 20, 30, 40, 60 min

4.3.1. Determination of Operational Parameters for RNIP

4.3.1.1. pH. The impact of pH was tested by sonication of 10 mg L^{-1} of chromium in the presence of RNIP for 30 minutes at varying pH values. Samples were collected at 10 min intervals for AAS analysis. The fraction of chromium removal at pH 3, 4 and 5 are presented in Figures 4.15.

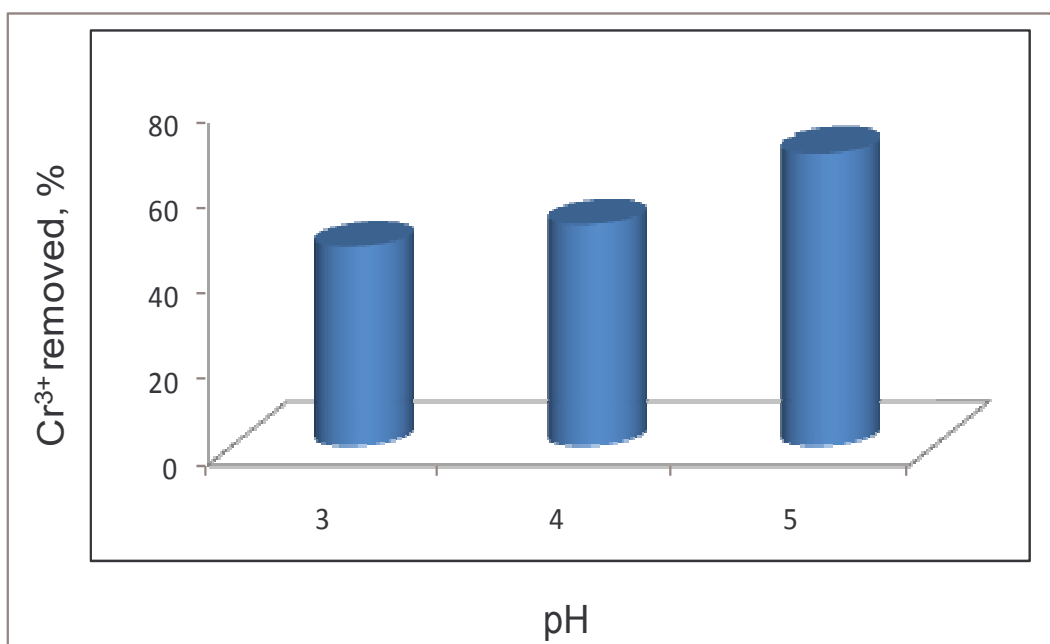


Figure 4.15. Effect of pH on chromium removal by ultrasound in the presence of RNIP.

It was observed that the maximum chromium removal was achieved at pH=5. On the other hand, the fraction of chromium removal was found to be slightly lower at pH=3. pH 5 was chosen as working pH for chromium removal by ultrasound in the presence of RNIP.

4.3.1.2. Contact Time. The impact of sonication duration was determined by monitoring the fraction of chromium removal at 10 min intervals. The data are presented in Figure 4.16.

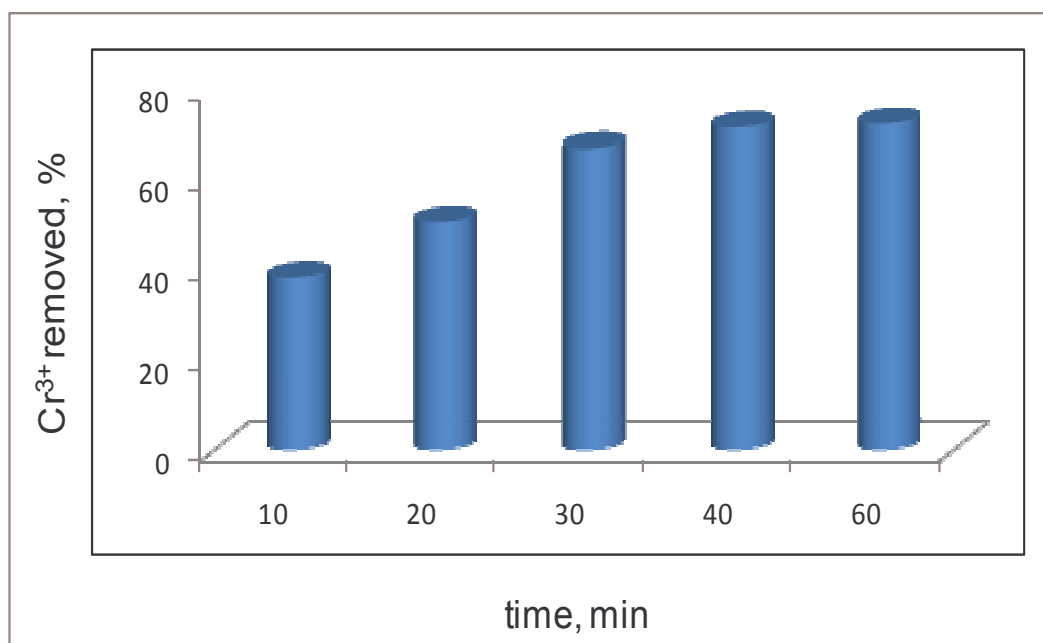


Figure 4.16. Optimization of contact time for Cr(III) removal by ultrasound in the presence of RNIP (20 g L⁻¹).

It was observed that 67 per cent chromium was removed in first 30 minutes, and the removal efficiency did not change too much. The contact time required for 67 per cent chromium removal by ultrasound in the presence of RNIP selected as 30 minutes.

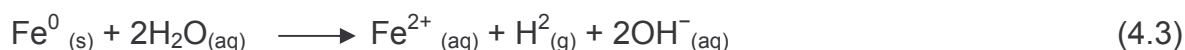
4.3.2. Determination of Operational Parameters for ZVI

The reaction chemistry expected to occur during the sonication of the solution in the presence of ZVI is as follows:

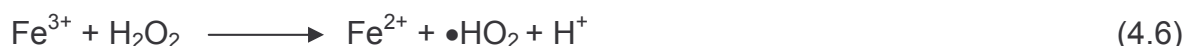
During the sonolysis of solution, the $\bullet\text{OH}$ radicals is formed to form hydrogen peroxide.



Upon the addition of ZVI, it is oxidized to a Fenton reagent Fe^{2+} from exposure to oxygen and water.



Decomposition of sonochemically produced H_2O_2 is accelerated through Fenton's reaction (Equation 4.4), resulting in the formation of additional $\bullet\text{OH}$ radicals.



The $\bullet\text{OH}$ thus formed either reacts with Fe(II) to produce Fe(III) or can react with, causes reduction of chemical oxygen demand and biochemical oxygen demand of solution mixtures.

4.3.2.1. pH. The impact of pH was tested by sonication of 10 mg L^{-1} of chromium in the presence of ZVI for 40 minutes at varying pH values. Samples were collected at 10 min intervals for AAS analysis. The fraction of chromium removal at pH 3, 4 and 5 are presented in Figure 4.17.

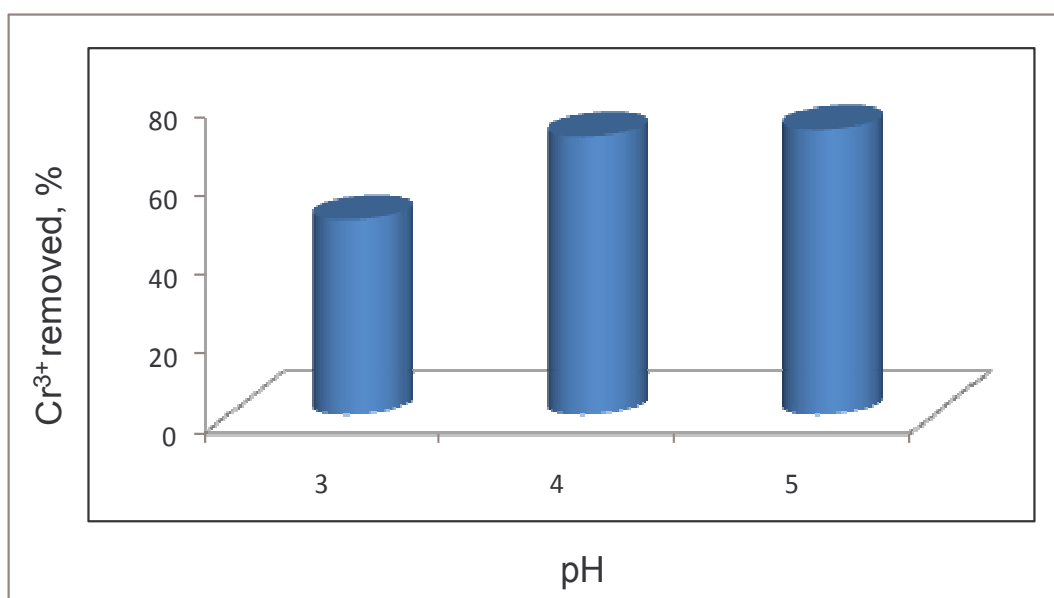


Figure 4.17. Effect of pH on the fraction of chromium removal by ultrasound in the presence of ZVI.

As can be seen from the data in Figure 4.17, the fraction of chromium removal is low at pH 3. However, it is equal at pH 4 and 5 as adsorption experiments in the presence of ZVI.

4.3.2.2. Contact Time. The impact of sonication duration was determined by monitoring the fraction of chromium removal at 10 min intervals. The data are presented in Figures 4.18.

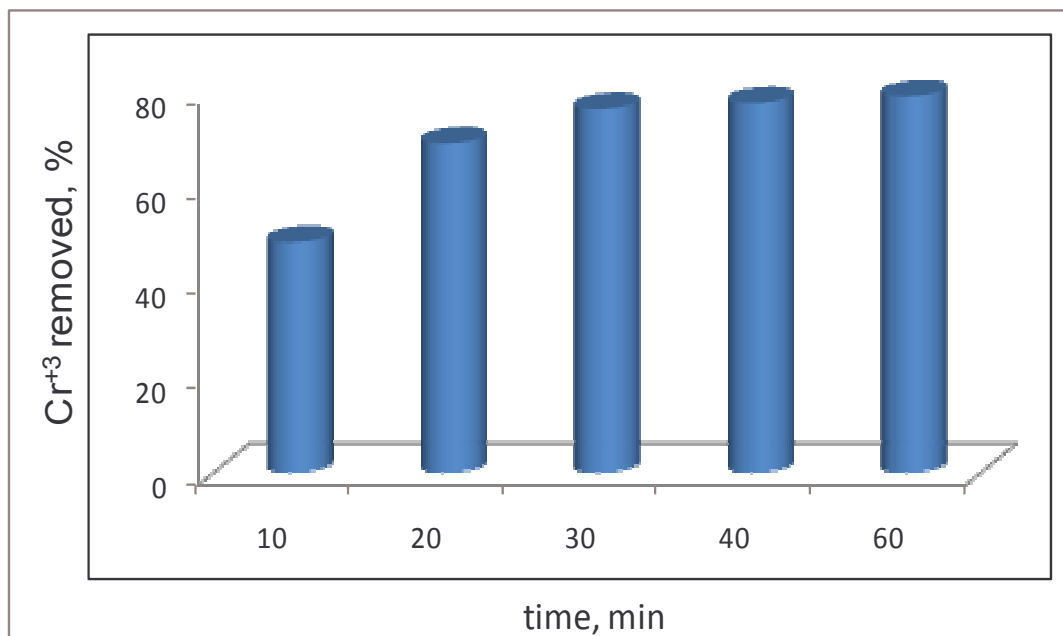


Figure 4.18. Optimization of contact time for Cr(III) removal by ultrasound in the presence of ZVI.

It was observed that approximately 50 per cent of chromium removed at first 10 minutes and the fraction of chromium removal did not change too much after 30 minutes. The contact time required for 76 per cent chromium removal by ultrasound in the presence of ZVI selected as 30 minutes.

4.3.2.3. Effect of Solution Matrix 1. The effect of solution matrix was investigated by adding organic matter as glucose to a chromium solution of 10 mg L^{-1} and running the adsorption experiments with ZVI at pH 4. The residual concentration of each was monitored during 20 minutes. The fraction of chromium and BOD_5 removal are presented in Figures 4.19. It was found that the fraction of chromium removal decreased with increasing BOD_5 and the fraction of BOD_5 removal just 29 % and 16% when initial BOD_5 equals to 100 mg L^{-1} and 200 mg L^{-1} , respectively.

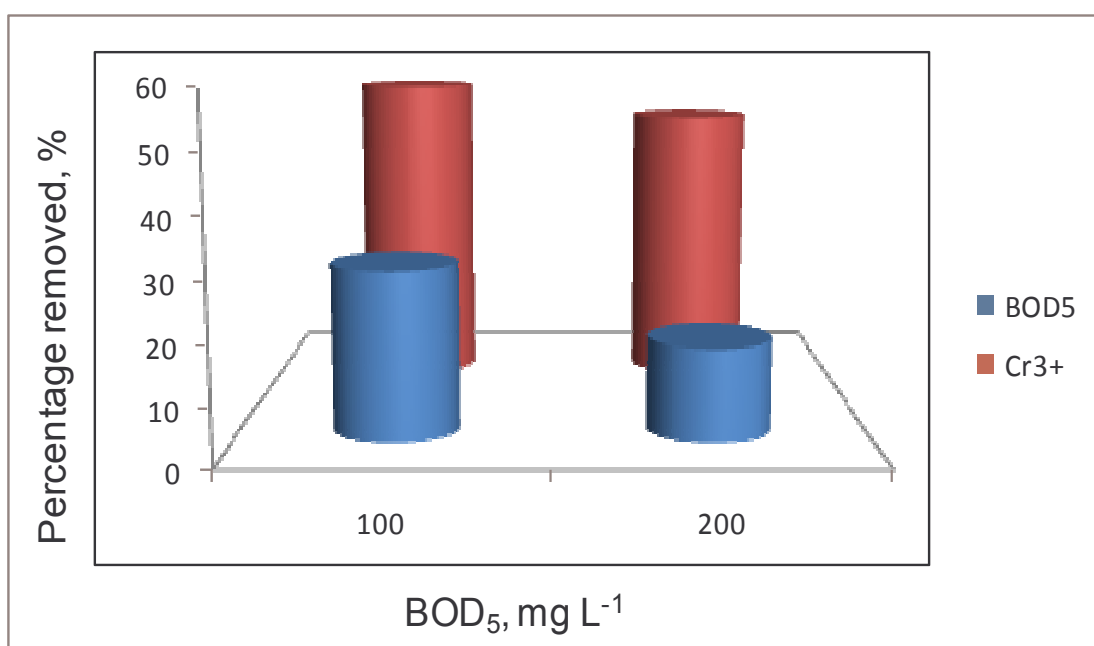


Figure 4.19. The fraction of chromium and BOD_5 removal by ultrasound in the presence of ZVI.

4.4. Comparison of Silent and Sonicated Adsorption Systems (Single Solution)

Operational parameters found for silent and sonicated systems in the presence of RNIP and ZVI are presented in Table 4.6 and Table 4.7, respectively.

Silent System

At the end of 2 hour adsorption, fraction of chromium removal in the presence of RNIP and ZVI was found 72 % and 79 %, respectively. It can be seen from the data in Table 4.6, the main difference between RNIP and ZVI is their optimum concentration to observe adsorption. When RNIP was added into solution less than 10 mg L⁻¹, adsorption of chromium did not observe very much.

Table 4.6 Operational Parameters for chromium (III) removal by adsorption of single solution in the presence of RNIP and ZVI.

Nanoparticle	Adsorbent concentration, mg L ⁻¹	Time, hour	pH	Fraction of chromium removal, %
RNIP	20	2	5	72
ZVI	0.6	2	5	79

Sonicated System

The data in Table 4.7 shows that chromium was removed from solution at a faster rate when the solution is sonicated. Solution needs to be sonicated 1 hour to achieve 72 % and 79 % chromium removal, in the presence of RNIP and ZVI, respectively.

The fraction of chromium removal is greater in the presence of ZVI than in the presence of RNIP at the end of 20 min sonication. Optimum pH was found 5 for both adsorbent as found in silent system.

Table 4.7. Operational Parameters for chromium (III) removal by sonication of single solution in the presence of RNIP and ZVI.

Nanoparticle	Adsorbent concentration, mg L⁻¹	Time, min	pH	Fraction of chromium removal
RNIP	20	20	5	51
ZVI	0.6	20	5	70

4.5. Comparison of Silent and Sonicated System (Solution Matrix 1)

Solution matrix 1 was prepared by adding organic matter as glucose to a chromium solution of 10 mg L^{-1} and running the adsorption experiments with ZVI at pH 4. Fractions of chromium and BOD₅ removal for silent and sonicated adsorption systems are presented in Table 4.8 and Table 4.9, respectively.

Silent System

Table 4.8. The fraction of chromium and BOD₅ removal by adsorption of solution matrix 1 (pH:4, ZVI: 0.6 g/L, t: 2 hour).

	Cr(III) removal, %	BOD ₅ removal, %
Cr(III): 10 mg/L	79	
Cr(III): 10 mg/L BOD ₅ : 100mg/L	43	26
Cr(III): 10 mg/L BOD ₅ : 200mg/L	41	17

Sonicated System

Table 4.9. The fraction of chromium and BOD₅ removal by sonication of solution matrix 1 (pH:4, ZVI: 0.6 g/L, t: 20 m).

	Cr(III) removal, %	BOD ₅ removal, %
Cr(III): 10 mg/L	70	-
Cr(III): 10 mg/L BOD ₅ : 100mg/L	56	29
Cr(III): 10 mg/L BOD ₅ : 200mg/L	50	16

4.6. Comparison of Silent and Sonicated System (Solution Matrix 2)

Solution matrix 2 was prepared by dissolving potassium chromium sulphate (Cr(III): 40 mg L⁻¹) in a stock solution of pluck that has 1000 mg L⁻¹ COD. The percentage of chromium, COD and BOD₅ removal for silent and sonicated system in the presence of ZVI are presented in Table 4.10 and Table 4.11, respectively.

Silent System

The fraction of chromium, COD and BOD₅ removal in solution mixture (100 mgL⁻¹ COD + 40 mgL⁻¹ Cr(III)) was found 59 % , 40 % and 26 % in the presence of ZVI. The fraction of chromium removal was found 79 % for single solution.

Table 4.10. The percentage of chromium, COD and BOD₅ removal by adsorption of solution matrix 2 (pH:4, ZVI: 0.6 g L⁻¹).

Time, min	Chromium Removal, %	COD Removal, %	BOD ₅ Removal,%
15	41	5	3
30	45	17	11
45	46	20	9
60	49	33	18
90	56	39	20
120	59	40	26
150	61	41	32
180	65	42	37

Sonicated System

Application of ultrasound to solution mixture prepared by mixing pluck that has 1000 mg L^{-1} COD and potassium chromium sulphate (Cr(III): 40 mg L^{-1}) in the presence of ZVI showed that 56 % chromium, 47 % COD and 26 % BOD₅ removed at the end of 20 min. The chromium removal was found 70 % for single chromium solution.

Table 4.11. The percentage of chromium, COD and BOD₅ removal by sonication of solution matrix 2 (pH: 4, ZVI: 0.6 g L^{-1}).

Time, min	Chromium removal, %	COD removal, %	BOD₅ removal,%
10	52	40	22
20	56	47	26
30	57.2	51	17
40	57.3	52	35
60	57.4	52	40

5. CONCLUSIONS

The purpose of this research was to investigate treatability of chromium(III) by adsorption on RNIP and ZVI and the enhancement in the process by sonication of the solution. Selection of Cr(III) was based on the fact that it is the major pollutant in tannery wastewater and very toxic. The method involved comparison of chromium removal in the presence of adsorbent in silent and sonicated adsorption systems and monitoring the residual chromium in test solutions at 357.9 nm. A summary of the main findings of the study is as the following:

1. The use of ZVI together with ultrasonic irradiation for Cr³⁺ removal is a potential method of wastewater treatment from tannery industries. The potential is due to good adsorbent qualities of iron and the power of ultrasound to enhance surface properties and to continuously clean the surfaces.
2. Removal of Cr³⁺ by ultrasound in the presence of ZVI is also a potential method since ZVI is a mild reducing agent and It is much more cost effective than salts of iron, which are used to produce Fenton Reaction.
3. The rate of chromium removal in the presence of RNIP is faster than in the presence of ZVI. However, ZVI (powder form) is more effective than RNIP (suspension form) in sonicated system due to the enhancement of ultrasound in surface purification.
4. Removal of chromium is mostly limited by mass transfer of chromium to the ZVI surface. Ultrasonic irradiation enhance that transport by causing transient cavitation results in turbulent flow conditions within the reactor.

6. When solution is sonicated in the presence of ZVI, heterogenous reactions occur in the reactor. The heterogenous reaction involves five steps;
 - a. Mass transfer of the chromium to the ZVI surface from the bulk solution.
 - b. Adsorption of chromium on the ZVI surface.
 - c. Oxidation-reduction reactions on ZVI surface
 - d. Over time, desorption of chromium from ZVI surface.
 - e. Mass transfer of chromium into the bulk solution.
7. Addition of ZVI into the solution resulted in an increase in the rate of chromium removal. This can be explained by Fe^{2+} ions released by oxidation of Fe^0 and the enhancement in OH radicals by the catalytic action of Fe^{2+} .
8. Due to the possibility of oxidation of Cr^{3+} to Cr^{6+} in sonicated system, Cr^{6+} was also measured. The results showed that there was no Cr^{6+} in solution. This could be resulted by reduction of Cr^{6+} by H radicals created by ultrasound. However, there must be a Cr^{3+} discharge limit for tannery wastewaters since Cr^{3+} could oxidize to Cr^{6+} in surface water.

REFERENCES

Adewuyi Y. G., 2001. Sonochemistry: Environmental science and engineering applications, *Industrial and Engineering Chemistry Research*, 40, 4681-4715.

Berlan, J., Mason, T. J., 1992. Sonochemistry: From Research Laboratories to Industrial Plants, *Ultrasonics*, 30, 203-212.

COWI, 2000. Bat notes for tanneries, institutional support to SCEP (Goskomekologiya)- Working paper No 31.

Deutsche Gesellschaft für Technische Zusammenarbeit (GTZ) GmbH, 1997. Environmental management guideline for the leather tanning and finishing industry, Thailand, PN 2000.2266.5-001.00.

Donmez, L.H., Kallenberger, W.E., 1989. Soil Leachate: Determination of hexavalent chromium, *Journal of the American Leather Chemists Association (JALCA)*, Vol. 86, pp.110-121.

Drijvers, D., Van Langenhove, H., Beckers, M., 1999. Decomposition of phenol and trichloroethylene by the ultrasound/H₂O₂/CuO process. *Water Research*, 33(5), 1187-1194.

European Society of Sonochemistry, <http://www.europeansocietysonochemistry.eu>

European Commission, February 2003. Integrated pollution prevention and control (IPPC) reference document on best available techniques for the tanning of hides and skins.

Fischer, C. H., Hart, E. J., Henglein, A., 1986. Ultrasonic irradiation of water in the presence of oxygen 18, ¹⁸O₂: isotope exchange and isotopic distribution of hydrogen peroxide. *Journal of Physical Chemistry*, 90, 1954-1956.

Guo, Z. R., Zhang, G., Fang, J., Dou, X., 2006. Enhanced chromium recovery from tanning wastewater, *Journal of Cleaner Production*, 75-79.

Heidemann, E., 1993. *Fundamentals of leather manufacturing*, Eduart Roether KG-D-64212 Darmstad, 1st edition.

Higham, R.D., 1994. *Low waste technology suitable for tanneries in developing economies*, UNIDO (UN Industrial Development Organization).

HMIP-Her Majesty's Inspectorate of Pollution-UK, 1995. *Guidance chief inspectors's guidance to inspectors-processing of animal hides and skins, process guidance note, IPR 6/7*.

Holister P., Weener, J. W., Vas, C. R., Harper, T., 2003. *Nanoparticles-Technology White Papers, No:3, 2-11*.

Hua I., Hoffmann M. R., 1997. Optimization of ultrasonic irradiation as an advanced oxidation technology. *Environmental Science and Technology*, 31, 2237-2243.

Ince, N. H., Tezcanli, G., 2001. Reactive dyestuff degradation by combined sonolysis and ozonation. *Dyes and Pigments*, 49, 145-153.

Ince, N. H., Tezcanli, G., Belen, R K., Apikyan, I. G., 2001. Ultrasound as a catalyzer of aqueous reaction systems: the state of the art and environmental applications. *Applied Catalysis B: Environmental*, 29, 167-176.

Ivanov, V., Tay, J.H., Tay, S.T., Jiang, H.L., 2004. Removal of micro-particles by microbial granules used for aerobic wastewater treatment. *Water Science and Technology* 50(12): 147-154.

Klabunde, K. J., Lagadic, I., Dieken, L., Boronina, T. N., 1998. Zinc-silver, zinc-palladium, and zinc-gold as bimetallic systems for carbontetrachloride dechlorination in water. *Journal of Hazardous Substance Research*, 1, 6.1-6.15.

Kontronarou, A., Mills, G., Hoffmann, M. R., 1991. Ultrasonic irradiation of p-nitrophenol in aqueous solution. *Journal of Physical Chemistry*, 95, 3630-3638.

Lepoint, T., Mullie, F., 1994. "What exactly is a cavitation chemistry", *Ultrasonics Sonochemistry*, 1, 13-22.

Makkino, K., Mossoba, M., Riesz, P., 1982. Chemical effects of ultrasound on aqueous solutions. *Journal of American Chemical Society*, 104 (12), 3537-3539.

Margulis, M.A., 1995, *Sonochemistry and Cavitation*, Gordon and Breach Publishers, ISBN 2-88124-849-7.

Mason, T. J., Lorimer, J.P., Walton, D.J., 1990. Sonoelectrochemistry. *Ultrasonics*, 28, 333-337.

Mason T. J., Lorimer J.P., 2002. *Applied Sonochemistry*, Wiley-VCH Verlag GmbH, ISBN 3-527-30205-0.

Mason, T. J., Cordemans, E.D., 1998. Practical consideration for process optimization, J. L. Luche (Ed), *Synthetic Organic Sonochemistry*, 301-331, Plenum Press.

Mason, T.J., 1999. *Sonochemistry*, Oxford University Press Inc., New York.

Moore, M. N., 2006. Do Nanoparticles present ecotoxicological risks for the health of the aquatic environment. *Environment International* 32(8), 967-976.

National Cleaner Production Centre, Achieving production effectiveness and increasing business competitiveness through cleaner production, P.K., Gupta, Director, 5-6 Institutional Area, Lodi Road, New Delhi-110 003, India.

The National Nanotechnology Initiative, <http://www.nano.gov/>

Nurmi, J. T., Tratnyek, P. G., Sarathy, V., Baer, D. R., Amonette, J. E., Pecher, K., Wang, C., Linehan, J. C., Matson, D. W., Penn, R. L., Driessen, M. D., 2005. Characterization and properties of metallic iron nanoparticles: spectroscopy, electrochemistry, and kinetics. *Environmental Science and Technology*, 39 (5), 1221-1230.

Oberdörster, G., Oberdörster, E., Oberdörster, J., 2005. Nanotoxicology: an emerging discipline evolving from studies of ultrafine particles. *Environmental Health Perspective*, 113 (7), 823-839.

Official Gazette, 1999. Water Pollution Control Regulations of Turkey, No:1.7/23742.

Pearson, R.P., Maguire M.D., Bowden, R.J., 1999. "BLC Information Document, Best Available Technologies".

Petrier, C., Lamy, M. F., Francony, A., Benahcene, A., David, B., 1994. Sonochemical degradation of phenol in dilute aqueous solutions: comparison of the reaction rates at 20 and 487 kHz. *Journal of Physical Chemistry*, 98, 10514-10520.

Pontius, F. W., 1990. *Water Quality and Treatment*, McGraw-Hill, Inc., U.S.A., pp. 781-785.

Raghava R., J., Chandrababu, N.K., Muralidharan, C., Unni Nair, B., Rao, P.G., Ramasami, T., 2003. Recouping the Wastewater: A way forward for cleaner leather processing, *Journal of Cleaner Production*, 591-599.

Reisse, J., 1995. Measurements of gas bubble sizes using high frequency ultrasound imaging, proceedings of the 15th international congress on acoustics, Trondheim, Norway, August 1995, 5, 409-412.

Riesz, P., Mason T. J., 1991. Advances in Sonochemistry, JAI Press, London, 23.

Sharphouse, J.H.,1971. Leather Technician's Handbook, Leather Producers' Association, UK.

Suslick, K. S., Hammerton, D. A., Cline, Jr., R. E., 1986. Sonochemical Hot Spot, Journal of American Chemical Society, 108, 5641-5642.

Suslick, K. S., 1990. Sonochemistry, Science, 247, 1439-1445.

Suslick K. S., 1994. The Chemistry of Ultrasound,
<http://www.scs.uiuc.edu/~suslick/britannica.htm>

United Nations Environment Programme (UNEP), 1991. Tanneries and the Environment, A Technical Guide to Reducing the Environmental Impact of Tannery Operations.

U.S. Environmental Protection Agency, 2007. Nanotechnology White Paper.

Weavers, L. K., Ling, F. H., Hoffmann, M. R., 1998. Aromatic compound degradation in water using a combination of sonolysis and ozonolysis. Environmental Science and Technology, 32, 2727-2733.

Weber, W. J., 1972. Physicochemical Processes for Water Quality Control, Wiley-Interscience, New York.

Wiesner, M. R., Lowry, G. V., Alvarez, P., Dionysiou, D., Biswas, P., 2006. Assessing the risks of manufactured nanomaterials. *Environmental Science and Technology*, 40 (14), 4336-4345.

World Bank Group, 2000. *Pollution Prevention and Abatement Handbook: Tanning and Leather Finishing*, Environment Department, Washington. D. C. The document available at;

[http://wbi0018.worldbank.org/essd.nsf/GlobalView/PPAH/\\$File/80_tan.pdf](http://wbi0018.worldbank.org/essd.nsf/GlobalView/PPAH/$File/80_tan.pdf).

Young, F.R., 1989. *Cavitation*, McGraw-Hill, New York,.

Zhang, W., 2003. Nanoscale iron particles for environmental remediation: An Overview. *Journal of Nanoparticle Research*, 5, 323-332.

Zhao G., Mingfang L., Zhonghua H., Huikang H., 2004. Dissociation and removal of complex chromium ions containing in dye wastewaters, *Separation Purification Technology* 43(2005) 227-232.

APPENDIX A**Calibration Curve of Chromium for AAS Analysis**

A series of chromium solution of 1, 2 and 4 mg L⁻¹ were injected to the AAS to achieve a calibration curve and it was used for the quantification of chromium as presented in Table A and Figure A.

Table A. Detected peak areas for the injected chromium solutions during calibration of AAS.

Chromium concentration, mg L ⁻¹	Absorbance at 357.9 nm
1	0.039
2	0.074
4	0.194

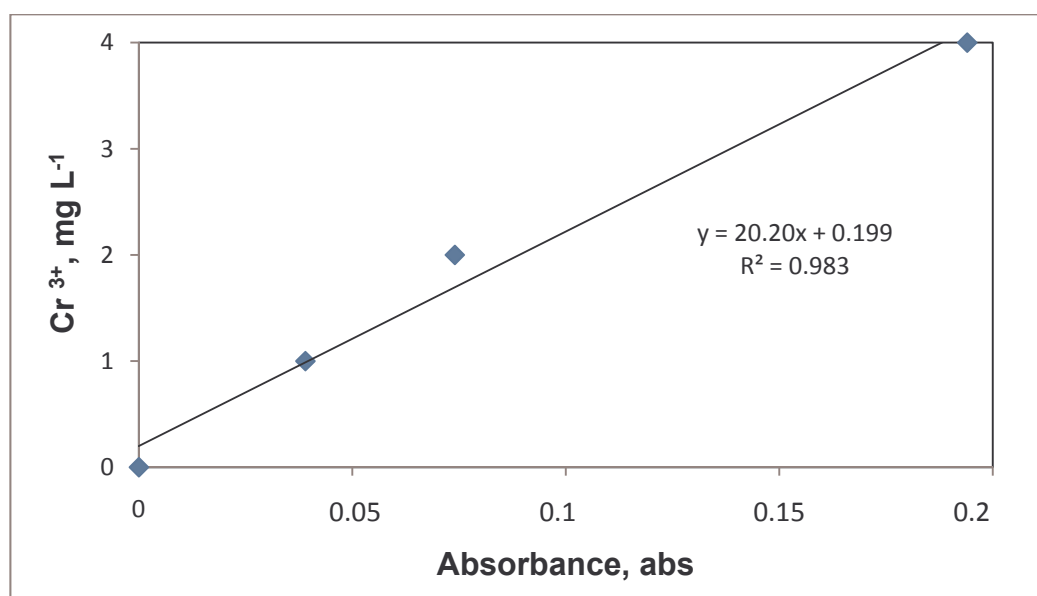


Figure A. Calibration curve of chromium for AAS analysis.

APPENDIX B

Calibration Curve of COD for Spectrophotometer Analysis

A series of KHP (potassium hydrogen phosphate) solutions of 50, 100, 200, 300, 400 and 500 mg L⁻¹ were injected to the spectrophotometer to achieve a calibration curve and it was used for the quantification of COD as presented in Table B and Figure B.

Table B Detected peak areas for the injected KHP solutions during calibration of spectrophotometer.

COD, mg L ⁻¹	Absorbance at 600 nm
50	0.018
100	0.041
200	0.073
300	0.12
400	0.141
500	0.186

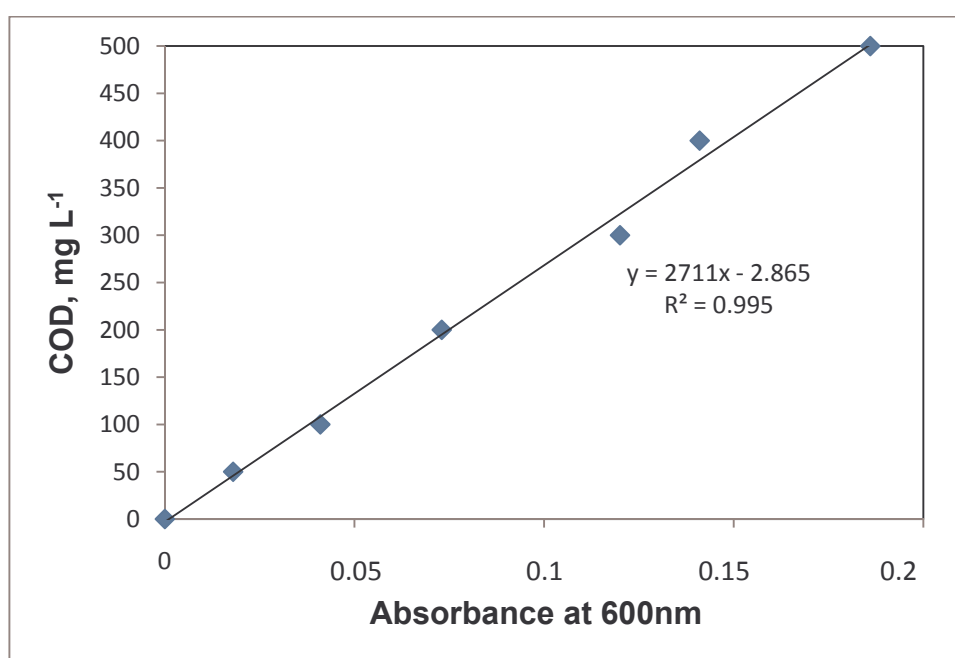


Figure B. Calibration curve of KHP solution for COD analysis.